

Linear and Non-Linear Analysis of SMA Based Duffing Oscillators

Gaikwad Shantanu Rajendra

A Thesis Submitted to
Indian Institute of Technology Hyderabad
In Partial Fulfillment of the Requirements for
The Degree of Master of Technology



Department of Mechanical and Aerospace Engineering

June 2016

Declaration

I declare that this written submission represents my ideas in my own words, and where ideas or words of others have been included, I have adequately cited and referenced the original sources. I also declare that I have adhered to all principles of academic honesty and integrity and have not misrepresented or fabricated or falsified any idea/data/fact/source in my submission. I understand that any violation of the above will be a cause for disciplinary action by the Institute and can also evoke penal action from the sources that have thus not been properly cited, or from whom proper permission has not been taken when needed.

S. P. Gaikwad

(Signature)

Gaikwad Shantanu Rajendra

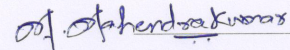
(Gaikwad Shantanu Rajendra)

ME14MTECH11024

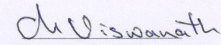
(Roll No.)

Approval Sheet

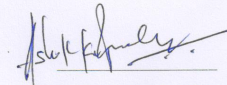
This Thesis entitled Linear and Non-Linear Analysis of SMA Based Duffing Oscillators by Gaikwad Shantanu Rajendra is approved for the degree of Master of Technology from IIT Hyderabad



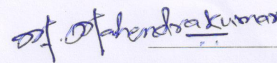
(Dr. Mahendrakumar Madhavan) Examiner
Dept. of Civil Eng
IITH



(Dr. Viswanath Chinthapenta) Examiner
Dept. of Mech Eng
IITH



(Dr. Ashok Kumar Pandey) Adviser
Dept. of Mech Eng
IITH



(Dr. Mahendrakumar Madhavan) Chairman
Dept. of Civil Eng
IITH

Acknowledgements

I would like to thank all the people who have guided and supported me throughout my thesis work. First of all, I express my immense gratitude to my advisor, Dr. Ashok Kumar Pandey, for giving me valuable guidance and directions throughout my thesis work. I also thank him for mentoring me in such an interesting field of shape memory alloy and believing in me during the research work.

I would like to extend my gratitude to my committee members who have made interesting and useful remarks during my thesis work. I also wish to thank Professor Raja Banerjee, H.O.D, Department of Mechanical and Aerospace Engineering, IIT Hyderabad, for his support during my M.Tech program and Professor U.B Desai, Director, IIT Hyderabad for their support in various ways. I acknowledge all the faculty members of Mechanical Engg. Dept., IIT Hyderabad, specially Dr. R. Prasanth Kumar, Dr. C. P. Vyasarayani, Dr. M. Ramji, Dr. B. Venkatesham, Dr. V. Chinthapenta for giving me valuable technical details in the subjects I studied during my course work. These techniques helped me directly or indirectly in completing my thesis work. I must not ignore the special contributions of the institute library for providing all the necessary books, articles and access to many useful domains to enrich my asset list in this research work.

Many, many thanks go to my family for their blessings and support. I wish to thank my father and mother for supporting me during my studies in various ways. I am also thankful to my IIT Hyderabad friends for the warmth of their friendship and providing a supportive environment, which has made my stay at IIT Hyderabad wonderful. I sincerely acknowledge my group mates Mukul, Vamsi Krishna, Sajal and for their role in supporting me indirect ways. I would also like to acknowledge Mr. Prashant Kambli and Ms. Aparna Gangele Ph.D. Scholars, IIT Hyderabad, for their support and help in giving suggestions for solving papers during the thesis work.

Dedication

To my Family and Teachers.

Abstract

Recently, there have been many applications involving shape memory alloy (SMA) to actuate or control small to large vibration in the field of aerospace, automobile, building structures, bioengineering devices, etc. The application of SMA over a wide field is due to its ability to apply large force and displacement with low power. It is also found that SMA can regain its original state after going through the cycle of heating and cooling processes. During the process of loading, the internal temperature change due to phase transformation which causes energy dissipation. Due to its effective energy dissipation capabilities, it can respond to slow loading, fast loading, sudden loading, and time varying loading, respectively. However, to understand the effective control of vibration of a structure, it is important to investigate its linear and nonlinear behavior under the different loadings conditions. In this thesis, we plan to investigate the linear and nonlinear response of SMA controlled cantiliver beam (spring) under different loading conditions. To do the study, we first present the thermomechanical constitutive model of SMA with a single degree of freedom system. Subsequently, we solve the equation to obtain linear frequency and nonlinear frequency response using the method of harmonic balance. To analyze the influence of cubic and quadratic nonlinearity, we modify the governing equation and discuss the results based on the method of harmonic balance. Additionally, we also describe the method of averaging to obtain the nonlinear frequency response of SMA based oscillators. The analysis of results lead to various ways of controlling the nature and extent of nonlinear response of SMA based oscillators. Such findings can be effectively used to control the external vibration of different systems.

Contents

Declaration	ii
Approval Sheet	iii
Acknowledgements	iv
Abstract	vi
Nomenclature	viii
1 Introduction	1
1.1 Motivation	2
1.2 Literature Survey	3
1.3 Outline of Thesis	4
2 Thermomechanical Model of Shape-Memory Devices	5
2.1 Mathematical Model	5
2.2 A Numerical Method: Harmonic Balance Solution	13
2.3 Result and Discussion	15
2.3.1 Isothermal Regime	15
2.3.2 Non-Isothermal Regime	17
2.4 Summary	19
3 Analysis of SMA Based Duffing Oscillators Model by Harmonic Balance Solution	20
3.1 Investigation of SMA Based Cubic Oscillator	20
3.1.1 Mathematical Model	20
3.1.2 A Numerical Method: Harmonic Balance Solution	21
3.1.3 Result and Discussion	21
3.2 Investigation of SMA Based Cubic and Quadratic Oscillators	23
3.2.1 Mathematical Model	23
3.2.2 A Numerical Method: Harmonic Balance Solution	24
3.2.3 Result and Discussion	24
3.3 Summary	26
4 Analysis of SMA Model by Method of Averaging	27
4.1 Mathematical Model	27
4.2 A Numerical Method: Method of Averaging	28
4.3 Result and Discussion	30

4.3.1	SMA Oscillator without Cubic Nonlinearity	30
4.3.2	SMA Oscillator with Cubic Nonlinearity	32
4.4	Summary	33
5	Conclusion and Future work	34
5.1	Conclusion	34
5.2	Future work	34
	References	35

Chapter 1

Introduction

Shape memory alloy (SMA) has been used to control vibration in various areas as its behavior and response can be controlled under various operating conditions. While, it is used as an actuator in aircraft, its application in commercial jet engines may reduce the weight, and hence, their efficiency. It is also used to make solenoids commonly found in automobiles, and in intelligent reinforced concrete, IRC, to detect the cracks in bridges and buildings. Recently, it is also being used in the area of medicine and optometry because of its suitable properties.

A typical SMA material shows pseudoelastic or superelastic behavior in which for a given external loading, its internal temperature changes with deformation due to phase transformation and heat exchange with the surrounding. The phase transformation between austenite (A) at higher temperature and martensite (M) at lower temperature can induce an exothermic $A \rightarrow M$ as well as endothermic $M \rightarrow A$ transformations due to loading and unloading, respectively. Such change in temperature can be modeled using the laws of thermodynamics. A typical SMA response is described by the displacement, velocity, phase transformation and the temperature. It also exhibit hysteresis behavior due to strong coupling between thermal and mechanical variables. Figure 1.1(a) shows the structure of phase transformation between austenite to martensite state. Such transformation can be achieved either by changing the temperature or deforming the material under external loading. For increase in temperature under a given loading, the twinned martensite state at low temperature can be converted into austenite state at higher temperature. On the otherhand, for a given temperature, twinned martensite state can be converted into detwinned martensite state (deformed state) under external loading. However, on heating the deformed state can be converted to austenite state and then back to original state by cooling the material. However, in pseudoelasticity, such transformation changes its internal temperature and causes energy dissipation without any external cooling and/or heating. Therefore, it can respond to slow loading, fast loading, transient loading, and time varying loading. Thus, we can state that change in internal temperature is due to the combined effect of phase transformation and heat exchange with surrounding. Figure 1.1(b) shows a detailed hysteresis loop due to internal changes in phase and temperature of SMA. It shows that during cooling process, austenite state (A) converted into twinned martensite (B) where the process of martensite transformation initiate. It transformed into final state of detwinned martensite phase (C) under loading. After releasing the load, material regains its shape through a linear process until stress becomes zero (D). At point D, the process of transformation to austenite state starts. Due to

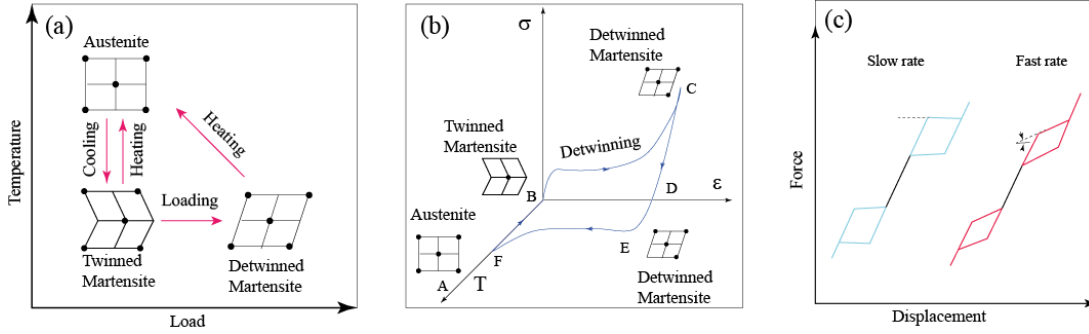


Figure 1.1: (a) Phase transformation of a SMA under loading and temperature effect; (b) Stress-strain-temperature hysteresis loop of a SMA; (c) Hysteresis loop at different loading rates.

heating process, such transformation completes at point F which is called the austenite phase.

SMA also shows the effect of superelasticity over a large elastic range. Under such condition, when mechanical load is applied, the alloy deforms reversibly to high strains by the formation of a stress-induced phase. When the mechanical load is removed, formation of new phase occur and it becomes unstable, and, thus, the material regains its original shape. Therefore, for a superelastic alloy, no change in internal temperature is needed to recover its original shape. However, SMA without superelastic effect require a change in internal temperature to recover a original shape. Figure 1.1(c) shows the effect of loading rate on hysteresis loop of SMA. It shows different types of responses under slow and fast loading and associated effects on the slopes of hysteresis loop. If loading rate is slow, temperature variations are small, hence the system shows isothermal condition. In isothermal process, the hysteresis loop is governed by the mechanical parameters only. Consequently, for a given sets of the mechanical parameters, the isothermal hysteresis loop is almost flat and the two plateaus are parallel. For faster loading rate, thermal effects become important. With consideration of high heat coefficient value, the system exchanges more heat with the environment. As a consequence, the plane in hysteresis loop is significantly different than the isothermal case. Consequently, under non-isothermal condition, the nearly flat plateaus become steeper and the area of the hysteresis loop is reduced. Therefore, to model a mechanical oscillator with SMA under external dynamic loading, the rate of loading needs to be taken into consideration. In this thesis, we discusses the response of SMA based oscillator with linear and nonlinear stiffness under isothermal as well as non-isothermal conditions.

1.1 Motivation

Most of the SMA based studies show the coupling of SMA and linear oscillator under isothermal and non-isothermal condition. They discuss ways to model nonlinear response specially due to the nonlinearity arising out of SMA behavior. However, there are hardly any study available which shows any coupling of SMA behavior with nonlinear oscillators. In this thesis, we present frequency response of SMA based on oscillator with cubic and quadratic nonlinear stiffness. The oscillator with cubic nonlinearity is termed as Duffing oscillator and that with quadratic nonlinear is termed as quadratic oscillator. A typical nonlinear response of a SMA shows nonlinear softening behavior. Since the Duffing oscillator may show nonlinear softening to nonlinear hardening response based on

the beam material, it can be used to tune the coupled response of SMA based nonlinear oscillator. Hence, it forms the motivation for presenting a systematic study of the coupled response of SMA based nonlinear oscillators with cubic and quadratic nonlinearity.

1.2 Literature Survey

With its peculiar memory effect, shape memory alloys have found many application in the fields of vibration control. The research related with the development of SMA material and tuning of its properties with new alloy for various application covers a wide range of problems. Dimitris [2] has discussed the modeling of SMA along with its application and properties in great detail. The commonly found shape memory alloys are Cu-based SMAs, shape memory ceramics, ferrous SMAs, NiTi SMAs, and shape memory polymers. However, the Ni-Ti alloy is used widely among others. They exhibit thermomechanical, thermoelectrical and thermochemical behavior under mechanical, thermal, electrical and chemical loading conditions. The pseudoelastic model of SMA is described vividly by Bernardini and Vestroni [3] using the single degree of freedom system. Many systems incorporating SMA based cantilever beam are also widely studied [3, 4, 5]. To study the thermomechanical behavior of SMA based system, the deformation, phase transformation and temperature variation are captured by the governing equation along with the constitutive equations of SMA. The constitutive equations governing hysteresis model are obtained using a free energy function as explained by Bernardini and Ivshin and Pence [6, 7] used for isothermal as well as non-isothermal conditions. The isothermal condition neglect the heat transfer with the surrounding [4]. Moussa et al. [8] presented the experimental as well as theoretical studies of the thermomechanical behaviour of superelastic shape memory alloys for quasi-static loading cases. Theoretical and experimental studies of SMA based system are also studied in varieties of structures [9, 10, 11]. The nonlinear frequency response of displacement amplitude as well as temperature in SMA based system is obtained by solving the coupled equation using the method of harmonic balance and averaging method, [12, 13, 14]. In addition to the model developed by [3], another micromechanical model is also developed by the Oberaigner et al. [18]. It consists of a kinetic equation, stress-strain relation, temperature-transformed and volume-fraction relations. These equations couple the heat conduction and the vibration of a rod. The change in phase of material leads to energy dissipation. Applying this model, a working temperature of damping can be found which lies between the temperatures of martensite start and the martensite finish. The thermodynamics of two models of pseudoelastic behavior of SMA are developed by Raniecki et al. [19]. The first model, R-model, undergoes reversible processes only and constitutes the Maxwell model of phase transformation. The second model, RL-model, includes interaction of energy. It determines formation of external and internal hysteresis loops with the Clausius-Duhem inequality. By using coupling of these models, we obtain the phase composition, stress-strain and heat exchange with surroundings environment.

Although, there are numerous studies available to analyze the influence of nonlinear frequency response of SMA based oscillator, but all of them consider nonlinearity directly associated with SMA behavior. In this thesis, we study the influence of cubic and quadratic nonlinearity on SMA based system. To do the analysis, we first consider the Duffing oscillator with cubic nonlinear nonlinearity [20]. We solve the equation using the method of harmonic balance. By varying the nature and strength of nonlinearity from softening to hardening [21], we obtain the coupled response of SMA

dased Duffing oscillator. Subsequently, we also analyze the combined effect of cubic and quadratic nonlinearity [22] using the method of harmonic balance. The above analysis is valid for isothermal as well as non-isothermal conditions. To compare different solution methods, we also solve SMA based Duffing oscillator using averaging method [23] for isothermal condition. On comparing the results obtained from the harmonic balance method and the methods of averaging, we found that the averaging method underestimate the solution due to numerical error [24]. The comparison of the solution of Duffing oscillator with and without SMA shows that the frequency tuning of SMA based response can be tuned effectively by varying the coefficients of Duffing and Quadratic oscillator.

1.3 Outline of Thesis

After giving fundamental details of SMA and literature related with its characterization in Chapter 1, we present detailed mathematical models for a SMA based oscillator by following the work of Lacarbonara et al. [4] in Chapter 2. To check the accuracy of governing equation and validate the solution approach, we reproduce the results of nonlinear frequency response of SMA based oscillator for the same set of parameters under isothermal and non-isothermal conditions. Additionally, we also validate our analytical solution with numerical results. In Chapter 3, we present the solution methodology using the method of harmonic balance to solve SMA based oscillator with additional cubic and quadratic nonlinear stiffness term. Subsequently, we discuss about the effect of different degrees of nonlinearity on frequency response of SMA based nonlinear oscillators, namely, Duffing and quadratic oscillators. In Chapter 4, we compare the solutions obtained by using the method of harmonic balance and the method of averaging for isothermal condition of SMA based oscillator with and without cubic nonlinearity. Finally, we present the concluding remarks and future work in Chapter 5.

Chapter 2

Thermomechanical Model of Shape-Memory Devices

In this chapter, we present complete mathematical modeling of thermomechanical behavior of SMA based oscillator by following the work done by Ivshin and Pence [7], Bernardini and Vestroni [3] and Lacarbonara et al. [4], respectively.

2.1 Mathematical Model

In SMA system, two cases taken into account for analysis: Isothermal and Non-isothermal. In the isothermal case, the dynamical system is three-dimensional as the state space is described by the displacement x , the velocity v , and the internal variable ξ which governs the evolution of the phase transformations that occur in the SMM [4]. In the non-isothermal case, the state space becomes four-dimensional as the temperature ϑ is added to x , v , and ξ in the state-space description [4].

The model of pseudoelastic oscillator contain mass m , damping system with damping coefficient μ , and SMA rod is shown in Figure 2.1(a). Figure 2.1(b) shows the description of heat exchange between the SMA with temperature ϑ and the surrounding with temperature ϑ_E . It also contain additional cubic and quadratic nonlinearity in stiffness. For the present analysis, we neglect this additional nonlinear effect. However, their effects will be discussed in details in Chapters 3 and 4. Here, the system is excited by harmonic force $F(t) = \gamma \cos(\Omega t)$. The harmonic force is balanced by pseudoelastic device (SMM) and damping system. Force produced by pseudoelastic device is f and by damping system is $\mu \dot{x}$, here x is displacement. During loading heat is exchanged with environment, ϑ_E is environment temperature and ϑ is the internal temperature of pseudoelastic device. The fraction of martensite phase in the device $\xi \in [0,1]$ is describe the evolution of the phase transformations [4]. When $\xi = 0$ the device is in a complete austenitic state (A) and when $\xi = 1$ the device is in a complete martensitic state (M). This effect is in the material microstructure and is taken into account by the material parameter δ with $\delta > 0$ representing the maximum transformation displacement [4].

Energy balance equation of thermomechanical system is given by

$$m\ddot{x} = \gamma \cos(\Omega t) - f - \mu \dot{x} \quad (2.1)$$

$$\dot{e} = f\dot{x} + \dot{Q} \quad (2.2)$$

$$\vartheta \dot{\eta} = \dot{Q} + \dot{\Gamma} \quad (2.3)$$

$$\dot{\Gamma} \geq 0 \quad (2.4)$$

where e denote the internal energy, \dot{Q} is the rate of heat exchange with the surrounding, $\dot{\Gamma}$ is the rate of energy dissipation, η is the entropy. Eq. (2.1) is the linear momentum balance, Eq. (2.2) is the internal energy balance and Eq. (2.3) and Eq. (2.4) are the balance of entropy and second law of thermodynamics [4].

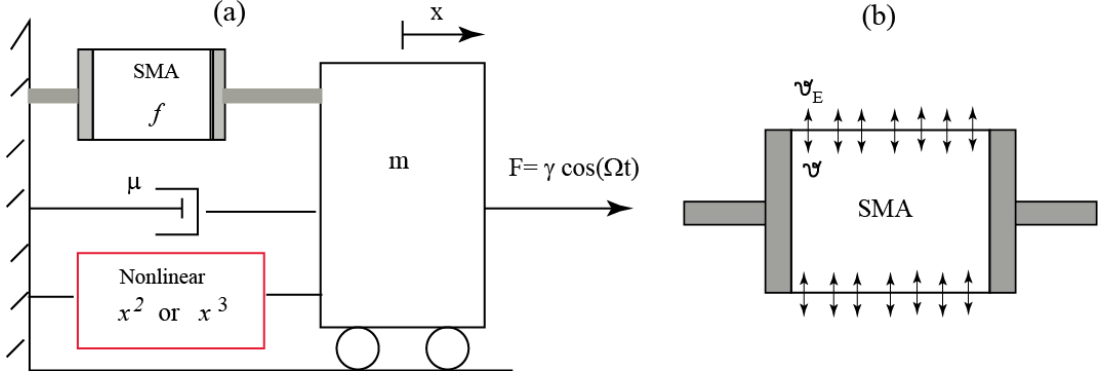


Figure 2.1: (a) A lumped model of SMA based oscillator including cubic and quadratic nonlinear stiffness. (b) A schematic of SMA with internal temperature and surrounding temperature.

Consider free energy function $\Phi = e - \vartheta\eta$ instead of internal energy e .

Using Eq. (2.2), Eq. (2.3) written as

$$\dot{\Phi} = f\dot{x} - \eta\dot{\vartheta} - \dot{\Gamma} \quad (2.5)$$

Equation \dot{Q} is the heat exchange between device and the surrounding. It is assumed that heat exchange due to convection, so by newtons law of heating

$$\dot{Q} = h(\vartheta_E - \vartheta) \quad (2.6)$$

where $h \geq 0$ is the heat exchange coefficient. Using Eq. (2.4) and Eq. (2.5) leads to

$$f = \frac{\partial \Phi}{\partial x}, \quad \eta = -\frac{\partial \Phi}{\partial \vartheta}, \quad \dot{\Gamma} = \Pi \dot{\xi} \geq 0 \quad (2.7)$$

where $\Pi = -\partial \Phi / \partial \xi$ is the thermodynamic force (driving force).

The following free energy function used in model [6, 7]

$$\Phi = \frac{K}{2}(x - \text{sgn}(x)\delta\xi)^2 + c(\vartheta - \vartheta_0 - \vartheta \ln \frac{\vartheta}{\vartheta_0}) + (\vartheta - \vartheta_0)b\delta\xi + a_0 - b_0\vartheta \quad (2.8)$$

where $K > 0$ is elastic stiffness, $c > 0$ is heat capacity, $b > 0$ is slope in the temperature transformation-force plane, a_0 and b_0 are internal energy and entropy of the device in the fully austenitic state at the reference temperature ϑ_0 [4]. The constitutive equation for the restoring force, entropy and thermodynamic force obtained from Eq. (2.7) and Eq. (2.8) as

$$f = \bar{f}(x, \vartheta, \xi), \quad \eta = \bar{\eta}(x, \vartheta, \xi), \quad \Phi = \bar{\Phi}(x, \vartheta, \xi)$$

$$f = \frac{\partial \Phi}{\partial x} = K(x - \text{sgn}(x)\delta\xi) \quad (2.9)$$

$$\eta = \frac{\partial \Phi}{\partial \vartheta} = c \ln \frac{\vartheta}{\vartheta_0} - b\delta\xi + b_0 \quad (2.10)$$

$$\Pi = \frac{\partial \Phi}{\partial \xi} = K\delta(|x| - \delta\xi) - b\delta(\vartheta - \vartheta_0) \quad (2.11)$$

In restoring force, Eq. (2.9), $\text{sgn}(x)\delta\xi$ is the pseudoelastic part of displacement.

The constitutive equation for $\dot{\xi}$ is the transformation kinetic so it state the evolution of the phase transformation [4].

$$\dot{\xi} = G(\Pi, \xi, \text{sgn}(\dot{\xi}))\dot{\Pi} \quad (2.12)$$

where G is the hysteresis controller.

$$G = \begin{cases} k_1(1 - \xi)[1 + \tanh(k_1\Pi + k_2)], & \text{if } \dot{\xi} > 0 \\ k_3\xi[1 - \tanh(k_3\Pi + k_4)], & \text{if } \dot{\xi} < 0 \end{cases} \quad (2.13)$$

The function G takes different equations of increasing or decreasing ξ in order to define the A \rightarrow M and M \rightarrow A transformations. The material parameters k_i can be taken from experimental data [4]. The integration of transformation kinetic used, to obtain the relationship between the phase fraction ξ and the driving force Π .

$$\xi = \begin{cases} \frac{1}{2} + \frac{1}{2} \tanh(k_1\Pi + k_2), & \text{Forward Transformation} \\ \frac{1}{2} + \frac{1}{2} \tanh(k_3\Pi + k_4), & \text{Reverse Transformation} \end{cases}$$

The true shape of the phase fraction evolution is regulated by k_1 (k_3 for the reverse transformation), which governs the slope of the transformation, and by k_2 (k_4 for the reverse transformation) which regulates the actual values of Π at which the transformation takes place [4].

$$\dot{\Pi} = K\delta(\text{sgn}(x)\dot{x} - \delta\dot{\xi}) - b\delta\dot{\vartheta}$$

$$\dot{\xi} = G\dot{\Pi} = -\frac{G\delta b}{1 + GK\delta^2}(\vartheta - \text{sgn}(x)\frac{K}{b}\dot{x}) \quad (2.14)$$

In Eq. (2.13) k_1 and $k_3 > 0$, means $G > 0$.

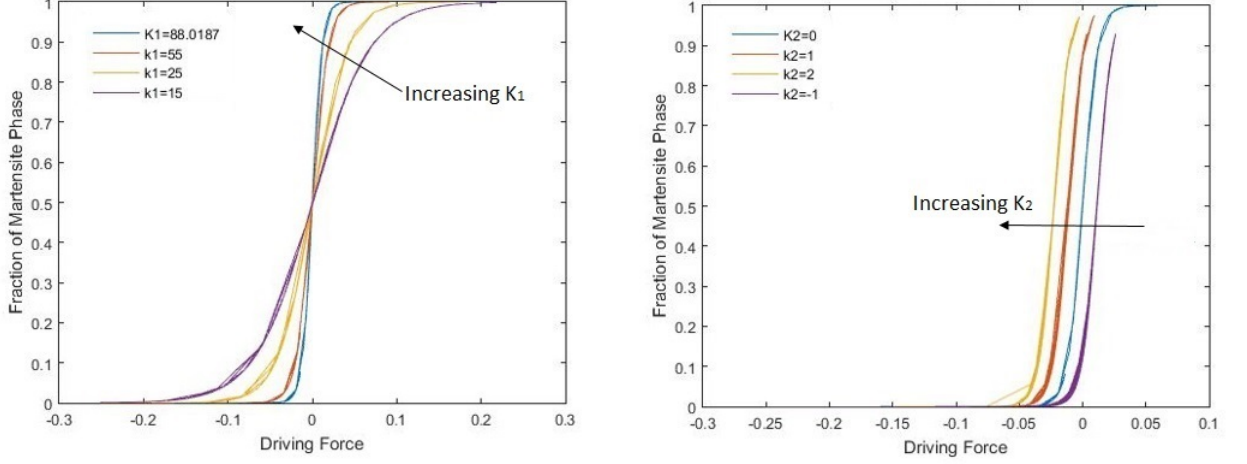


Figure 2.2: Effect of the parameters k_1 and k_2 on the evolution of ξ in terms of Π

In order to show the kinetic effect on the force-displacement behavior, consider a loading case, quasistatic force $F(t)$ at constant temperature $\vartheta(t) = T$ [4]. F can be written as a function of f ,

$$|F| = \text{sgn}(x)f = K(|x| - \delta\xi)$$

Driving force can also be written as a function of F ,

$$\Pi = \delta|F| - b\delta(\vartheta - \vartheta_0)$$

So expression of the force-displacement loading curve for forward transformation as

$$Kx = F + K\delta\xi$$

here $\xi = \frac{1}{2} + \frac{1}{2} \tanh(k_1\Pi + k_2)$, and at reference temperature $\vartheta(t) = \vartheta_0$, so $\Pi = \delta|F|$.

$$x = \frac{F}{K} + \frac{\delta}{2}(1 + \tanh(|F|k_1\delta + k_2))$$

The forces f_{Ms} and f_{Mf} , at which the forward transformation starts and finishes and ξ_r is the residual martensite at the conventional start of the transformation, for convenience take $r := \tanh^{-1}(1 - 2\xi_r)$ [4]. At constant temperature,

$$\xi_r = \frac{1}{2} + \frac{1}{2} \tanh(k_1\delta f_{Ms} - b\delta k_1(T - \vartheta_0) + k_2)$$

$$1 - \xi_r = \frac{1}{2} + \frac{1}{2} \tanh(k_1\delta f_{Mf} - b\delta k_1(T - \vartheta_0) + k_2)$$

Above two equation yields respectively,

$$k_1 \delta f_{Ms} - b \delta k_1 (T - \vartheta_0) + k_2 = -r$$

$$k_1 \delta f_{Mf} - b \delta k_1 (T - \vartheta_0) + k_2 = r$$

Solving for k_1 and k_2 ,

$$k_1 = \frac{-2r}{\delta(f_{Ms} - f_{Mf})}, \quad k_2 = r - 2r \frac{b(T - \vartheta_0) - f_{Mf}}{f_{Ms} - f_{Mf}}$$

The forces f_{As} and f_{Af} , at which the reverse transformation starts and finishes [4].

At constant temperature,

$$1 - \xi_r = \frac{1}{2} + \frac{1}{2} \tanh(k_3 \delta f_{As} - b \delta k_3 (T - \vartheta_0) + k_4)$$

$$\xi_r = \frac{1}{2} + \frac{1}{2} \tanh(k_3 \delta f_{Af} - b \delta k_3 (T - \vartheta_0) + k_4)$$

Above two equation yields respectively,

$$k_3 \delta f_{As} - b \delta k_3 (T - \vartheta_0) + k_4 = r$$

$$k_3 \delta f_{Af} - b \delta k_3 (T - \vartheta_0) + k_4 = -r$$

Solving for k_3 and k_4 ,

$$k_3 = \frac{-2r}{\delta(f_{Af} - f_{As})}, \quad k_4 = r - 2r \frac{b(T - \vartheta_0) - f_{As}}{f_{Af} - f_{As}}$$

Substitute the constitutive equation for $f, \eta, \dot{\Gamma}$ and \dot{Q} in Eq. (2.3) and solve by considering Z_1 and Z_2 as,

$$Z_1 = \frac{b \delta G}{1 + K \delta^2 G}, \quad Z_2 = -K \delta (|x| - \delta \xi) - \vartheta_0 b \delta$$

Driving force, $\Pi = K \delta (|x| - \delta \xi) - b \delta (\vartheta - \vartheta_0) = -Z_2 - b \delta \vartheta$

Entropy $\eta = c \ln \frac{\vartheta}{\vartheta_0} - b \delta \xi + b_0$

By solving entropy balance equation yield,

$$c \dot{\vartheta} + Z_2 \dot{\xi} = h(\vartheta_E - \vartheta) \tag{2.15}$$

By solving Eq. (2.14) yield,

$$\dot{\xi} + Z_1 \dot{\vartheta} = Z_1 \frac{K}{b} \text{sgn}(x) \dot{x} \quad (2.16)$$

Solving Eq. (2.15) and Eq. (2.16) simultaneously obtained equations for rate of temperature and rate of fraction of martensite as,

$$\dot{\xi} = \frac{Z_1}{c - Z_1 Z_2} [\text{sgn}(x) \frac{Kc}{b} v + h(\vartheta - \vartheta_E)] \quad (2.17)$$

$$\dot{\vartheta} = \frac{1}{c - Z_1 Z_2} [-\text{sgn}(x) \frac{K}{b} Z_1 Z_2 v - h(\vartheta - \vartheta_E)] \quad (2.18)$$

Added the equation of motion Eq. (2.1) in order to obtain the system of equation that describes the non-isothermal dynamics of the pseudoelastic device [4]. Consider $\dot{x} = v$, and express pseudoelastic force f in Eq. (2.1) and rearrange as the system reduced to a first-order explicit form $\dot{\mathbf{x}} = f(x, t)$, that is,

$$\dot{x} = v,$$

$$\dot{v} = \frac{\gamma}{m} \cos(\Omega t) - \frac{K}{m} (x - \text{sgn}(x) \delta \xi) - \frac{\mu}{m} v,$$

$$\dot{\xi} = \frac{Z_1}{c - Z_1 Z_2} [\text{sgn}(x) \frac{Kc}{b} v + h(\vartheta - \vartheta_E)],$$

$$\dot{\vartheta} = \frac{1}{c - Z_1 Z_2} [-\text{sgn}(x) \frac{K}{b} Z_1 Z_2 v - h(\vartheta - \vartheta_E)] \quad (2.19)$$

In order to capture the essential features of the response, set of Eqs. (2.19) has been written in a non-dimensional form by assuming, reference condition, the A \rightarrow M transformation at the temperature ϑ_r [4]. In such conditions force and displacement are denoted by f_{Ms} and x_{Ms} , with $f_{Ms} = Kx_{Ms}$. The temperature ϑ_r is the value at which the device exhibits pseudoelastic response. Variables with hat denotes the non-dimensional form. Arrange Eq. (2.19) in non-dimensional form as,

$$\dot{\hat{x}} = \hat{v}$$

$$\dot{\hat{v}} = \hat{\gamma} \cos(\hat{\Omega} \hat{t}) - (\hat{x} - \text{sgn}(\hat{x}) \lambda \hat{\xi}) - 2\zeta \hat{v}$$

non-dimensional form for Z_1 and Z_2 are,

$$\hat{Z}_1 = \frac{\hat{G}}{1 + \lambda J \hat{G}}, \quad \hat{Z}_2 = -L[J(|\hat{x}| - \lambda \hat{\xi}) + \hat{\vartheta}_0]$$

The evolution of phase transformation can be described in non-dimensional form as,

$$\dot{\xi} = \frac{\hat{Z}_1}{1 - \hat{Z}_1 \hat{Z}_2} [\text{sgn}(\hat{x}) J \hat{v} + \hat{h}(\hat{\vartheta} - \hat{\vartheta}_E)]$$

The rate of temperature change of pseudoelastic device can be written in non-dimensional form as,

$$\dot{\vartheta} = \frac{1}{1 - \hat{Z}_1 \hat{Z}_2} [-\text{sgn}(\hat{x}) J \hat{Z}_1 \hat{Z}_2 \hat{v} - \hat{h}(\hat{\vartheta} - \hat{\vartheta}_E)]$$

Rearrange the equations of system in normal form (non-dimensional form) as,

$$\dot{\hat{x}} = \hat{v},$$

$$\dot{\hat{v}} = \hat{\gamma} \cos(\hat{\Omega} \hat{t}) - (\hat{x} - \text{sgn}(\hat{x}) \lambda \xi) - 2\zeta \hat{v},$$

$$\dot{\xi} = \frac{\hat{Z}_1}{1 - \hat{Z}_1 \hat{Z}_2} [\text{sgn}(\hat{x}) J \hat{v} + \hat{h}(\hat{\vartheta} - \hat{\vartheta}_E)],$$

$$\dot{\vartheta} = \frac{1}{1 - \hat{Z}_1 \hat{Z}_2} [-\text{sgn}(\hat{x}) J \hat{Z}_1 \hat{Z}_2 \hat{v} - \hat{h}(\hat{\vartheta} - \hat{\vartheta}_E)] \quad (2.20)$$

where the non-dimensional variables [4],

$$\hat{t} = \omega t, \quad \hat{x} = \frac{x}{x_{Ms}}, \quad \hat{\vartheta} = \frac{\vartheta}{\vartheta_r},$$

$$\hat{G} = G b \delta \vartheta_r, \quad \hat{Z}_1 = \frac{\hat{G}}{1 + \lambda J \hat{G}} = \vartheta_r Z_1, \quad \hat{Z}_2 = -L [J(|\hat{x}| - \lambda \xi) + \hat{\vartheta}_0] = \frac{Z_2}{\vartheta_r c} \quad (2.21)$$

with $\omega^2 = \frac{K}{m}$ and the non-dimensional parameters [4] are

$$\lambda = \frac{\delta}{x_{Ms}}, \quad L = \frac{b\delta}{c}, \quad \hat{h} = \frac{h}{c\omega}, \quad J = \frac{f_{Ms}}{b\vartheta_r}, \quad \hat{k}_j = k_j b \delta \vartheta_r, \quad j = 1, 3$$

$$\zeta = \frac{\mu}{2\omega m}, \quad \hat{\gamma} = \frac{\gamma}{f_{Ms}}, \quad \hat{\Omega} = \frac{\Omega}{\omega} \quad (2.22)$$

The kinetic parameters \hat{k}_i do not have a direct physical meaning, they can be expressed in terms \hat{q}_i , parameter \hat{q}_i possess a physical meaning [4]. These \hat{q}_i parameters are defined as

$$\hat{q}_1 = \frac{f_{Mf}}{f_{Ms}}, \quad \hat{q}_2 = \frac{f_{Af}}{f_{As}}, \quad \hat{q}_3 = \frac{f_{As}}{f_{Ms}}$$

where f_{Ms} , f_{Mf} , f_{As} , and f_{Af} are the forces at the start and finish of the associated transformations

at the reference temperature ϑ_r [4]. The relations between the \hat{k} 's and \hat{q} 's are

$$\hat{k}_1 = \frac{2r}{J(\hat{q}_1 - 1)}, \quad \hat{k}_2 = k_2 = \frac{2(1 - \hat{\vartheta}_0) - J(\hat{q}_1 + 1)}{J(\hat{q}_1 - 1)}r$$

$$\hat{k}_3 = \frac{2r}{(1 - \hat{q}_2)\hat{q}_3J}, \quad \hat{k}_4 = k_4 = \frac{2(1 - \hat{\vartheta}_0) - \hat{q}_3J(\hat{q}_2 + 1)}{(1 - \hat{q}_2)\hat{q}_3J}r$$

To obtain upper and lower pseudoelastic plateaus with the same force variation, the condition $f_{Mf} - f_{Ms} = f_{As} - f_{Af}$ used [4]. Using this condition obtained the \hat{q}_2 as,

$$\hat{q}_2 = \frac{1 + \hat{q}_3 - \hat{q}_1}{\hat{q}_3}$$

Moreover, b is the slope in the transformation force–temperature plane [4]. Stress free transformation temperature, $M_s, M_f, A_s,$ and A_f are the temperatures at the start and finish of the associated transformations [4]. The change of temperatures at the start and finish of the associated transformations are,

$$M_s = 1 - J; \quad M_f = 1 - J\hat{q}_1; \quad A_s = 1 - J\hat{q}_3; \quad A_f = 1 - J\hat{q}_2\hat{q}_3.$$

Temperature in free energy ϑ_0 is the mean value of the stress-free transformation temperatures [4].

$$\Delta\vartheta_{M_s} = \vartheta_r - \vartheta_{M_s} = \vartheta_r M_s, \quad \Delta\vartheta_{M_f} = \vartheta_r - \vartheta_{M_f} = \vartheta_r M_f$$

$$\Delta\vartheta_{A_s} = \vartheta_r - \vartheta_{A_s} = \vartheta_r A_s, \quad \Delta\vartheta_{A_f} = \vartheta_r - \vartheta_{A_f} = \vartheta_r A_s$$

Collecting the values of $\Delta\vartheta_{M_s}, \Delta\vartheta_{M_f}, \Delta\vartheta_{A_s}$ and $\Delta\vartheta_{A_f}$ in terms of M_s, M_f, A_s and A_f respectively, ϑ_0 can be expressed as,

$$\vartheta_0 = \frac{\Delta\vartheta_{M_s} + \Delta\vartheta_{M_f} + \Delta\vartheta_{A_s} + \Delta\vartheta_{A_f}}{4}$$

$$\hat{\vartheta}_0 = 1 - J \frac{1 + \hat{q}_1 + \hat{q}_3 + \hat{q}_2\hat{q}_3}{4}$$

non-dimensional form of driving force,

$$\hat{\Pi} = \frac{\Pi}{b\delta\vartheta_r} = \frac{Kx_{M_s}}{b\vartheta_r}(|\hat{x}| - \lambda\xi) - (\hat{\vartheta} - \hat{\vartheta}_0)$$

non-dimensional form of hysteresis controller is,

$$\hat{G} = \begin{cases} \hat{k}_1(1 - \xi)[1 + \tanh(\hat{k}_1\hat{\Pi} + \hat{k}_2)], & \text{if } \dot{\xi} > 0 \\ \hat{k}_3\xi[1 - \tanh(\hat{k}_3\hat{\Pi} + \hat{k}_4)], & \text{if } \dot{\xi} < 0 \end{cases}$$

non-dimensional form of restoring force of pseudoelastic device is,

$$\hat{f} = \frac{f}{f_{Ms}} = \hat{x} - \text{sgn}(\hat{x})\delta\xi$$

Hence, non-dimensional variables and parameters will be considered and hat will be neglected for ease of notion.

2.2 A Numerical Method: Harmonic Balance Solution

The investigation of SMA damping system followed two type of responses: time response curve and frequency response curve. To capture a behavior of system in time response curves, integrate the set of Eqs. (2.20) using numerical integration and obtained a value of each variable for every second and plot the graph of each variable with time scale. We used MATLAB software for numerical integration and plotting of graphs.

In order to investigate the system behavior, in this thesis, harmonic balance solution method is used to plot frequency response curves. Harmonic balance method is used to calculate and analyze the steady-state response of nonlinear differential equations. It is a frequency domain method used for investigating the responses. The algorithm of harmonic balance is a special version of Galerkin's method. It is used to calculate the periodic solutions of autonomous and non-autonomous differential-algebraic systems of equations. In frequency response curve Ω is a control parameter. From above constitutive equations (Eqs. (2.20)) three variables x , ϑ and ξ causes non-linear motion of oscillator. Arrange the constitutive equations as follows,

$$\begin{aligned} \ddot{x} &= \gamma \cos(\Omega t) - (x - \text{sgn}(x)\lambda\xi) - 2\zeta\dot{x}, \\ \dot{\vartheta} &= h(\vartheta_E - \vartheta) - Z_2\dot{\xi} \end{aligned} \quad (2.23)$$

Let,

$$\mathbf{X} = \begin{bmatrix} \ddot{x} \\ \dot{\vartheta} \end{bmatrix}$$

and consider,

$$\begin{aligned} L_1 &= \gamma \cos(\Omega t) - (x - \text{sgn}(x)\lambda\xi) - 2\zeta\dot{x}, \\ L_2 &= h(\vartheta_E - \vartheta) - Z_2\dot{\xi} \end{aligned}$$

so \mathbf{X} can be written as,

$$\mathbf{X} = \begin{bmatrix} \ddot{x} \\ \dot{\vartheta} \end{bmatrix} = \begin{bmatrix} L_1 \\ L_2 \end{bmatrix} \quad (2.24)$$

Now assume Fourier series for variables as follows,

$$\begin{aligned}
x &= \frac{a_0}{2} + \sum_{i=1}^N A_n \cos(n\Omega t) + B_n \sin(n\Omega t) & n = 1, 2, \dots, N \\
\vartheta &= \frac{b_0}{2} + \sum_{i=1}^N C_n \cos(n\Omega t) + D_n \sin(n\Omega t) & n = 1, 2, \dots, N \\
L_1 &= \frac{c_0}{2} + \sum_{i=1}^N E_n \cos(n\Omega t) + F_n \sin(n\Omega t) & n = 1, 2, \dots, N \\
L_2 &= \frac{d_0}{2} + \sum_{i=1}^N H_n \cos(n\Omega t) + I_n \sin(n\Omega t) & n = 1, 2, \dots, N
\end{aligned} \tag{2.25}$$

Solving Eq. (2.24) and set of Eqs. (2.25) obtained,

$$\begin{aligned}
E_n + A_n \Omega^2 &= 0 \\
F_n + B_n \Omega^2 &= 0 \\
H_n - D_n \Omega &= 0 \\
I_n + C_n \Omega &= 0
\end{aligned} \tag{2.26}$$

In set of Eqs. (2.26), $4N$ unknown, A_n , B_n , C_n and D_n and $4N$ equations. The Fourier coefficients E_n , F_n , H_n and I_n are depends on A_n , B_n , C_n and D_n . To calculate Fourier coefficients E_n , F_n , H_n and I_n use the iterative algorithm based on evolution of A_n , B_n , C_n and D_n . From Fourier coefficients of A_n , B_n , C_n and D_n calculate values of x and ϑ for timespan of $[0, \frac{2\pi}{\Omega}]$. Using values of x and ϑ obtained the values of ξ by using numerical integration. Obtained the values of L_1 and L_2 using values of x , ϑ and ξ . Finally, calculate the values of E_n , F_n , H_n and I_n by using IFFT (Inverse Fast Fourier Transform) [3]. In order to obtained a unstable branch of frequency response curve used arc continuation method. Here, spherical arclength continuation method is used to obtained a constrained equation. The constrained equation are as follows,

$$(\mathbf{x} - \mathbf{x}_i)^T (\mathbf{x} - \mathbf{x}_i) - (\Delta s)^2 = 0$$

Here, \mathbf{x} is unknown quantity of current step and \mathbf{x}_i known quantity of previous step. In above constrained equation s is arclength along a curve and Δs is step size. In this thesis, predictor-

corrector algorithm is used for iterative method. Here, secant predictor algorithm used and proposed as following,

$$\mathbf{x}_{i+1} = \mathbf{x}_i + p_i(\mathbf{x}_i - \mathbf{x}_{i-1})$$

Where, p_i is step-dependent parameter. For corrector algorithm used Newton-Raphson iterative method and by using predictor-corrector method obtained values of unknown constant.

2.3 Result and Discussion

In this section, we present the transient as well as frequency response of SMA based simple oscillator under two different conditions, namely, isothermal and non-isothermal conditions.

2.3.1 Isothermal Regime

The isothermal case deals with constant temperature so $\dot{\vartheta} = 0$, using Eq. (2.20), the heat exchange rate with the surrounding environment is given by,

$$\dot{\vartheta} = \frac{1}{1 - Z_1 Z_2} [-\text{sgn}(x) J Z_1 Z_2 v - h(\vartheta - \vartheta_E)] = 0$$

$$\dot{Q} = h(\vartheta_E - \vartheta) = \text{sgn}(x) J Z_1 Z_2 v$$

substituting the obtained expression for \dot{Q} into Eq. (2.20) yields,

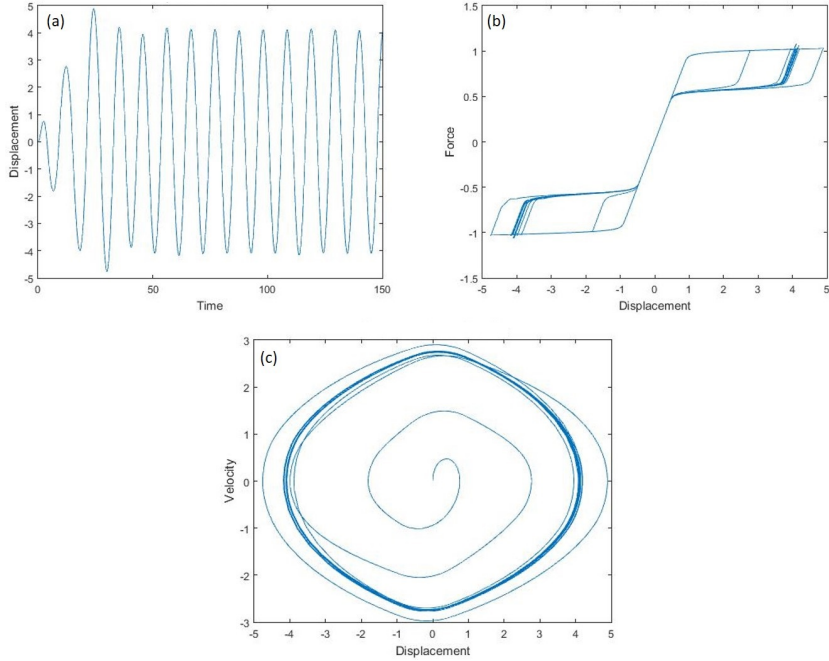


Figure 2.3: (a) Displacement vs Time (b) Force vs Displacement (c) Velocity vs Displacement

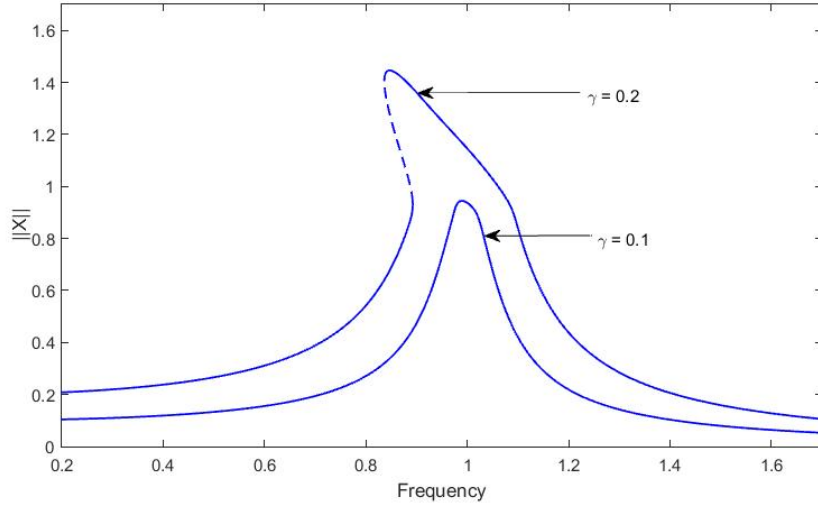


Figure 2.4: Frequency response curves of displacement for isothermal case

$$\dot{\xi} = JZ_1 \text{sgn}(x)v$$

Now, set of constitutive equations becomes as following,

$$\dot{x} = v,$$

$$\dot{v} = \gamma \cos(\Omega t) - (x - \text{sgn}(x)\lambda\xi) - 2\zeta v,$$

$$\dot{\xi} = JZ_1 \text{sgn}(x)v \quad (2.27)$$

The response of the system to harmonic excitations of various amplitudes has been computed through harmonic balance method as mentioned in above section. The range of amplitude is $\gamma = 0.1 - 0.6$ and $\Omega = 0.1 - 0.6$. In isothermal condition the material parameters taken from Lacarbonara et al.[4].

$$\lambda = 7; \quad \zeta = 0.05; \quad J = 0.315; \quad h = 0.08; \quad \vartheta_r = 293\text{K};$$

$$q_1 = 1.05; \quad q_3 = 0.6; \quad \vartheta_E = 293\text{K}; \quad \xi_r = 0.2; \quad L = 0.124.$$

For $\gamma = 0.6$ and $\omega = 0.6$ and taking initial condition $\mathbf{x}_0 = [0 \ 0 \ 0 \ 1]$, and integrating set of Eqs. (2.27), responses are describes in Figure 2.3. It is found that, after a few periods, the displacement tends to a symmetric periodic solution with zero mean value. That means it controls the vibration. In pseudoelastic effect, it forms the hysteresis loop. It stores the energy with loading and dissipate with temperature change, so it can stand with large deformation. It shows two hysteresis loop relating with tension and compression. In hysteresis loop plateaus are flat and parallel. Plot of displacement vs velocity shows that system oscillates around equilibrium point ($x = 0, v = 0$). To construct the frequency response curves, the non-dimensional frequency Ω is used as the control

parameter. In Figure 2.4, $\|x\|$ indicates the maximum value of the displacement attained over one cycle. Procedure of harmonic balance is used as mentioned in above section for obtained frequency response curves. Continuous lines except dotted lines denote stable solutions. The frequency response curves are, as expected, of the softening type thus mean a decrease of the frequency with the oscillation amplitude. In this thesis obtained a displacement frequency response curve for $\gamma = 0.1$ and $\gamma = 0.2$ only. For $\gamma = 0.1$ curve shows nearly linear response and maximum value of $\|x\|$ obtained at $\Omega = 0.1$. For higher force $\gamma = 0.2$ curve shows softening nature. Here resonance frequency shifts to left side means less than one. Above result and discussion also mentioned in [3, 4].

2.3.2 Non-Isothermal Regime

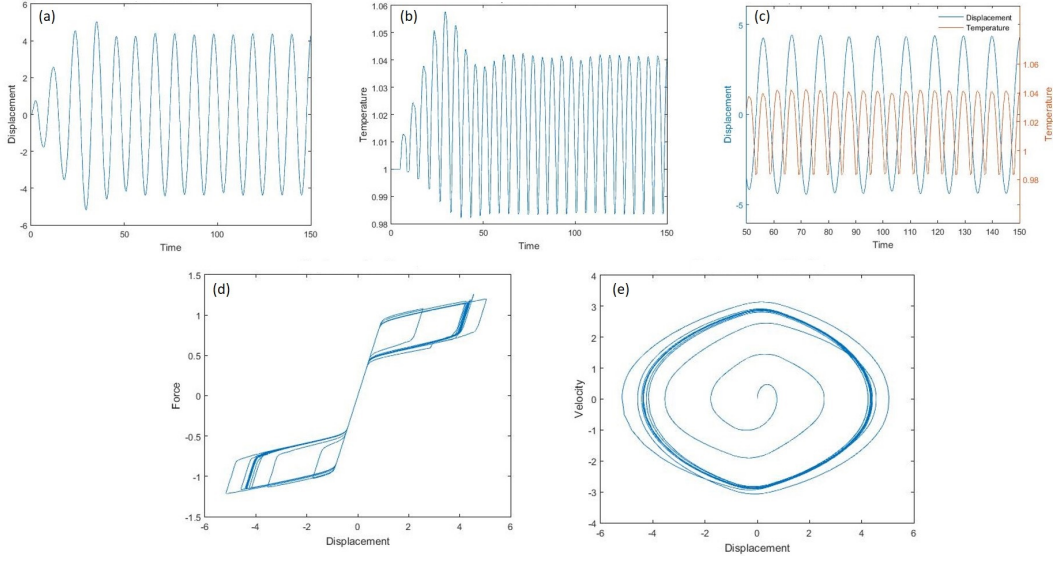


Figure 2.5: (a) Displacement vs Time (b) Temperature vs Time (c) Last 10 periods of displacement and temperature (d) Force vs Displacement (e) Velocity vs Displacement

As explained in Chapter 1, shape-memory devices interact thermodynamically with the external environment so that non-isothermal conditions occur. These materials under dynamic loading exhibit strong thermomechanical coupling with an influence on the mechanical response as shown in this section. In non-isothermal condition $\dot{\vartheta} \neq 0$, so the equations governing behavior of the system including thermodynamics are given by the full set in Eqs. (2.20), including the temperature as a state variable. The same parameters as used in the last isothermal case are considered. However, three additional parameters are to be considered, namely L , J and h . Concerning the non-dimensional temperature scale, the dimensional temperature is expressed in Kelvin (K). For example, the environmental temperature is 20°C (293 K), then a small increase of the non-dimensional temperature of 5% (i.e., $\theta = 1.05$) corresponds to a temperature variation of about 73% in $^\circ\text{C}$ [4]. The response of system are described in Figure 2.5 with reference to $\gamma = 0.6$, $\Omega = 0.6$ and initial conditions $\mathbf{x}_0 = [0 \ 0 \ 0 \ 1]$ while integrating Eq. (2.20). It is found that (Figure 2.5(a)), after a few periods, the displacement tends to a symmetric periodic solution with zero mean value. On the other hand, after a slightly longer transient, the temperature tends to a periodic solution with non-zero mean value. The mean temperature is greater than one. It indicating that, in this case, the total energy balance

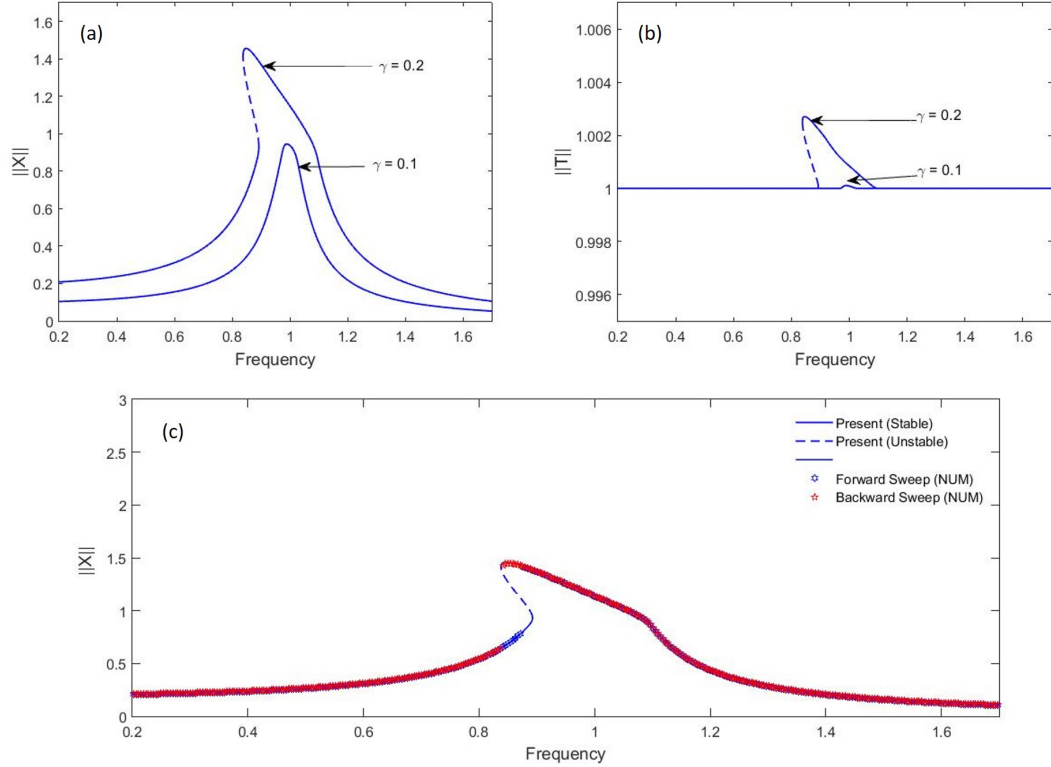


Figure 2.6: (a) Frequency response curves of displacement for non-isothermal case (b) Frequency response curves of temperature for non-isothermal case (c) Validation of result of harmonic balance solution by jump phenomenon for $\gamma = 0.2$

leads to an overheating of the device with respect to the environment temperature (Figure 2.5(b)). As from graphs, the frequency of the temperature is double because of two phase transformations cycles, one in tension and one in compression, correspond to a single displacement cycle. Phase transformations contribute to the temperature variations via the term $Z_2 \dot{\xi}$ (Eq. (2.15)) that depends on the absolute value of the displacement. Temperature variations during the oscillations are influenced by two factors: the amount of phase fraction transformed during the cycle, which relates with the maximum displacement, and the loading rate, which relates with the frequency. It is found that, temperature variations are found to increase with the maximum displacement and with the frequency and vice versa.

However, while for the displacement and temperature a plot of the maximum value versus the excitation frequency contains the basic information. The maximum displacement frequency curves for excitation amplitudes for 0.1 and 0.2 and responses are reported in Figure 2.6(a). Here, however, the response is govern by the temperature evolution and therefore the maximum frequency response curves are reported in Figure 2.6(b). Here when the maximum displacement is less than 1 hence there is no phase transformation, the response is linear elastic and the temperature is constant, i.e. the device remains at the surrounding environment temperature. The maximum temperature increases with the frequency decreases due to the significant maximum displacement rise. It turns out that, in this case, the effect of the transformation amount remains on that one of the loading rate and governs the temperature variations. Nature of displacement and temperature is softening

type same as isothermal case.

The maximum temperature response, shown in Figure 2.6(b), also exhibits that resonance frequency shifts to less than one. The temperature variations occur due to loading rate effect, so that the temperature decreases with the frequency. In peak region, two solutions related with complete phase transformation cycles are found for the same frequency. These solutions are characterized by the same transformed amount and by the same loading rate. During elastic loading and unloading heat exchange with the surrounding environment without any heat production. Hence the solution with greater maximum displacement can exchange with the surrounding environment more heat than the other solution. So it observed that loading rate and deformation significantly affect temperature and phase transformation. Above result and discussion also mentioned in [3, 4].

The results obtained in non-isothermal case by using harmonic balance solution are validated by numerical method as shown in Figure 2.6(c). In numerical result only stable part can obtained and for unstable part it take jump. The jump phenomenon are used to validate result of displacement frequency response curve for amplitude of excitation is $\gamma = 0.2$. The jump phenomenon is exactly matching with solution of harmonic balance method.

2.4 Summary

The characteristic of SMA device is studied through constitutive equations. The constitutive equations are in non-dimensional form. Using non-dimensional parameters, obtained a frequency response curves by the harmonic balance method. The SMA device with damping modeled for both isothermal and non-isothermal cases. The hysteresis loops indicate the effect of loading rate. In isothermal case temperature is constant but temperature variation in non-isothermal case for SMA device plotted in 2-D space of frequency and amplitude of temperature response. The responses of isothermal exhibit the theoretical situation but responses of non-isothermal exhibit the practical situation.

Chapter 3

Analysis of SMA Based Duffing Oscillators Model by Harmonic Balance Solution

In this Chapter, we discuss the influence of cubic and quadratic nonlinearity on the coupled response of SMA based oscillators as shown in Figure 2.1. Here, we first present solution methodology and analysis for cubic nonlinearity and then for the combined quadratic and cubic nonlinearity under non-isothermal conditions.

3.1 Investigation of SMA Based Cubic Oscillator

The Duffing oscillator is governed by Duffing equation, $\ddot{x} + \delta\dot{x} + \beta x + \alpha x^3 = \gamma \cos(\Omega t)$ [20] which contain cubic nonlinearity in stiffness. To analyze the behavior of SMA based Duffing oscillator, we obtain frequency response curves by using the harmonic balance method [22].

3.1.1 Mathematical Model

To analyze the SMA based Duffing oscillator, we add a cubic non-linear term $C_1 x^3$ in the governing equation given by Eqn. (2.1) as,

$$m\ddot{x} = \gamma \cos(\Omega t) - f - \mu\dot{x} - C_1 x^3$$

Solving the above non-dimensional form of the equation, we obtain,

$$\ddot{x} = \gamma \cos(\Omega t) - (x - \text{sgn}(x)\lambda\xi) - 2\zeta\dot{x} - \beta_0 x^3$$

where, $\beta_0 = \frac{C_1 x_{Ms}^3}{f_{Ms}}$. C_1 is Duffing coefficient. β_0 is a non-dimensional Duffing coefficient. It decide the dominance of Duffing oscillator in response of system. Rewritting the constitutive equations with Duffing oscillator in the state-space form, we get,

$$\dot{x} = v,$$

$$\dot{v} = \gamma \cos(\Omega t) - (x - \text{sgn}(x)\lambda\xi) - 2\zeta v - \beta_0 x^3,$$

$$\dot{\xi} = \frac{Z_1}{1 - Z_1 Z_2} [\text{sgn}(x)Jv + h(\vartheta - \vartheta_E)],$$

$$\dot{\vartheta} = \frac{1}{1 - Z_1 Z_2} [-\text{sgn}(x)JZ_1 Z_2 v - h(\vartheta - \vartheta_E)]. \quad (3.1)$$

The above constitutive equations are solved to obtain the frequency response curves of the system.

3.1.2 A Numerical Method: Harmonic Balance Solution

In order to investigate the system behavior follow a harmonic balance method. In frequency response curve Ω is a control parameter. In Duffing oscillator β_0 is a non-dimensional parameter, so value of it affect significantly on response of system.

Arrange the constitutive equations (Eqs. (3.1)) in following form,

$$\ddot{x} = \gamma \cos(\Omega t) - (x - \text{sgn}(x)\lambda\xi) - 2\zeta\dot{x} - \beta_0 x^3,$$

$$\dot{\vartheta} = h(\vartheta_E - \vartheta) - Z_2 \dot{\xi} \quad (3.2)$$

So using set of Eq. (3.2) follow a harmonic balance method as mentioned in Chapter 2 and obtained a harmonic balance equations. Using that equations obtained a frequency response curves for displacement and temperature.

3.1.3 Result and Discussion

In model SMA has nonlinear behavior due to energy dissipation capability. Duffing oscillator has cubic non-linearity. Combine of these two oscillator shows a peculiar behavior. To analyze this behavior obtained a frequency response curves for both displacement and temperature. For investigating behavior of Duffing oscillator due to incorporating SMA device, make comparison between two system through displacement frequency response curves. Two system: Duffing oscillator and Duffing oscillator with SMA device. The material of SMM device keep as Ni-Ti alloy.

In non-isothermal regime temperature changes with respect to time $\dot{\vartheta} \neq 0$, so it consider a thermodynamic parameter as given by Eq. (3.2). SMM material have strong coupling between thermal and mechanical parameters. The same value of parameters used as mentioned in isothermal case of shape memory devices. The Duffing oscillator added to SMA device and due to Duffing oscillator behavior of SMA device affected. The cubic non-linearity of Duffing oscillator affect on both displacement and temperature behavior of system. The response of Duffing oscillator is defined by $\beta_0 x^3$ term so value of β_0 has significant impact on response of system. Addition of Duffing oscillator in system of SMA device produce complex behavior. Investigation of this complex behavior is useful in industrial applications. Such a complex response captured in frequency response curves and resonance frequency of system is observed.

In SMA damping system frequency response curves shows softening nature for both displace-

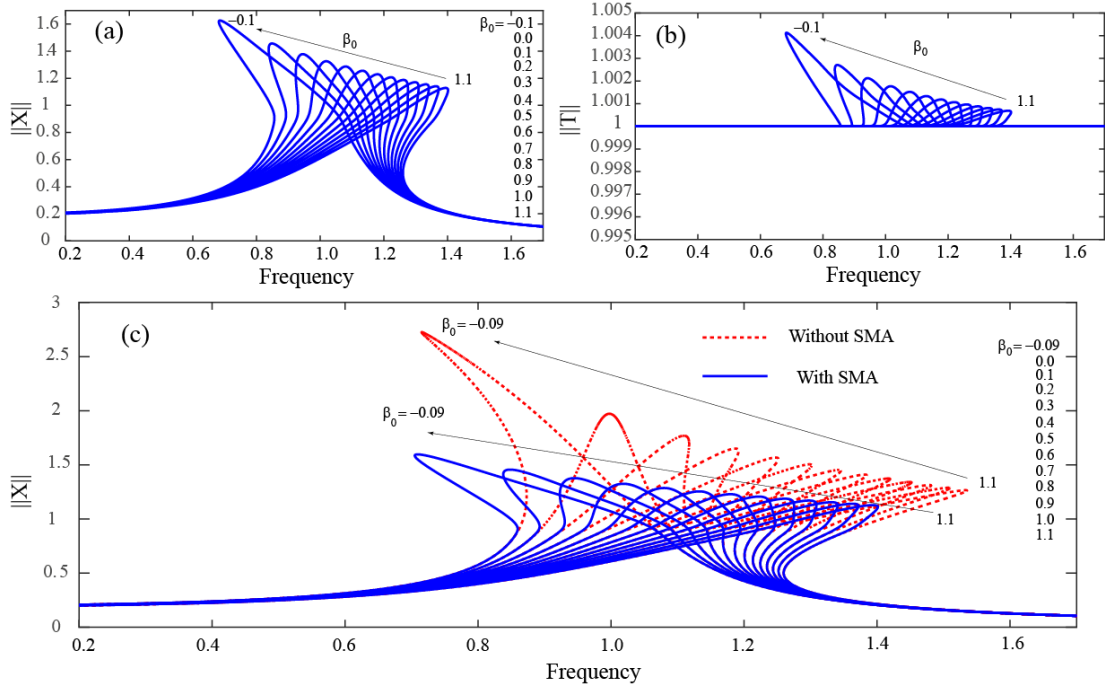


Figure 3.1: (a) Frequency response curves of SMA based cubic oscillator for displacement in non-isothermal case (b) Frequency response curves of SMA based cubic oscillator for temperature in non-isothermal case (c) Comparison of frequency response curves of displacement between cubic oscillator with SMA and without SMA

ment and temperature. Addition of Duffing oscillator affects maximum values of displacement and temperature which are obtained from time response curves. Duffing coefficient define the behavior of Duffing oscillator [21]. So Duffing oscillator affect the energy dissipation capacity and its dominance in non-linear region. Trough energy dissipation Duffing oscillator also affect heat exchange with surrounding environment and temperature cycle. So amount of heat exchange with surrounding affected due to phase transformation. The sign of Duffing coefficient has significant impact on response of system. So with respect to sign of Duffing coefficient Duffing oscillator changes its response. The response of Duffing oscillator governed by sign of Duffing coefficient which decide to support SMA effect or neutralize it. In this thesis, range of Duffing coefficient (β_0) is from -0.1 to 1.1. If value of β_0 is less than zero then it shows the supporting behavior of Duffing oscillator to SMA device and if β_0 is more than zero then it shows Duffing oscillator neutralize the effect of SMA oscillator. It also observed that with the change of β_0 value from negative to positive, maximum value of displacement and temperature decreases with frequency parameter. In frequency response curves, turning point (bifurcation point) shifts towards higher values of frequency with higher values of β_0 . For $\beta_0 = 0.1$ frequency response curve shows very small non-linearity of softening nature and for $\beta_0 = 0.2$ bifurcation point disappears for softening curve and become linear. This effect shown by both displacement and temperature frequency response curve as shown in Figure 3.1(a) and Figure 3.1(b). For $\beta_0 = 0.3$ curve becomes hardening curve and shows very small non-linearity. After that with increase of β_0 value non-linearity also increases. So with higher values of β_0 hardening types means increase of $\|X\|$ and $\|T\|$ with frequency and after bifurcation point values of $\|X\|$ and $\|T\|$ decreases with decrease of frequency (Figure 3.1(a) and Figure 3.1(b)). At $\beta_0 = 1.1$ frequency

response curve shows very less SMA damping effect and full dominance of Duffing oscillator.

In Duffing oscillator, influence of Duffing coefficient is same as shown with SMA device. The comparison is done only between displacement frequency responses. Here, range of β_0 is -0.09 to 1.1. In Figure 3.1(c) red color curves indicate the response of Duffing oscillator and blue color curves indicate the response of Duffing oscillator with SMA device. In Duffing oscillator, if value of β_0 is less than zero indicate softening nature of frequency response curves, with $\beta_0 = 0$ indicate linear nature and if β_0 is higher than zero indicate hardening nature. But for making comparison between Duffing oscillator and Duffing oscillator with SMA device, it is found that SMA system affect on Duffing oscillator in three cases: softening, linear and hardening nature of frequency response curve. The SMA system support the softening nature, so for $\beta_0 = -0.09$ frequency response curve shows softening nature. It is also found that linear curve in Duffing oscillator shift from $\beta_0 = 0$ to $\beta_0 = 0.2$ in Duffing oscillator with SMA device system. Simultaneously position of bifurcation point also changes and shifted towards downward. In Duffing oscillator with SMA device value of $\|X\|$ is decreases compare to Duffing oscillator system. For hardening nature, some higher values of β_0 used to neutralize SMA effect i.e up to $\beta_0 = 0.2$. At $\beta_0 = 0.2$ Duffing oscillator neutralize SMA effect and for $\beta_0 = 0.3$ and higher values of β_0 Duffing oscillator with SMA device system shows hardening nature. Continue increases in β_0 values, dominance of Duffing oscillator increases over SMA device.

3.2 Investigation of SMA Based Cubic and Quadratic Oscillators

The behavior of SMA device analyze in Chapter 2. The behavior of quadratic oscillator is govern by a non-linear second-order differential equation [25]. This behavior is defined by $\beta_1 x^2$ term. The quadratic oscillator has quadratic non-linearity. For the purpose of industrial applications complex system would set to control the vibration of structures. The Investigation of such complex behavior and combine effect of Duffing oscillator and quadratic behavior on SMA device is important. The behavior of Duffing oscillator is govern by Duffing equation. In this section obtained a mathematical model including Duffing and quadratic oscillators. To analyze the behavior of system obtained a frequency response curves by using harmonic balance method [22]. Investigate the results and make a discussion on that.

3.2.1 Mathematical Model

The model contain a SMA device, Duffing oscillator and quadratic oscillator. This system is excited by harmonic forcing. The behavior of SMA device added combine influence of cubic non-linearity and quadratic non-linearity. To add Duffing response in system, term $C_1 x^3$, and for quadratic response, term $C_2 x^2$ are incorporate in basic equation. Now Eq. (2.1) become,

$$m\ddot{x} = \gamma \cos(\Omega t) - f - \mu\dot{x} - C_1 x^3 - C_2 x^2$$

solving above equation for non-dimensional form and obtained,

$$\ddot{x} = \gamma \cos(\Omega t) - (x - \text{sgn}(x)\lambda\xi) - 2\zeta\dot{x} - \beta_0 x^3 - \beta_1 x^2$$

where, $\beta_0 = \frac{C_1 x_{Ms}^3}{f_{Ms}}$ and $\beta_1 = \frac{C_2 x_{Ms}^2}{f_{Ms}}$. C_2 is a quadratic coefficient. In above equation β_0 and β_1 are non-dimensional Duffing coefficient and quadratic coefficient respectively. Both coefficient have significant importance in investigation.

Arrange constitutive equations with Duffing and quadratic oscillators as following,

$$\begin{aligned}\dot{x} &= v, \\ \dot{v} &= \gamma \cos(\Omega t) - (x - \text{sgn}(x)\lambda\xi) - 2\zeta v - \beta_0 x^3 - \beta_1 x^2, \\ \dot{\xi} &= \frac{Z_1}{1 - Z_1 Z_2} [\text{sgn}(x)Jv + h(\vartheta - \vartheta_E)], \\ \dot{\vartheta} &= \frac{1}{1 - Z_1 Z_2} [-\text{sgn}(x)JZ_1 Z_2 v - h(\vartheta - \vartheta_E)]\end{aligned}\tag{3.3}$$

These constitutive equations used to obtained a response curves of system.

3.2.2 A Numerical Method: Harmonic Balance Solution

In order to investigate the system behavior follow a harmonic balance method. In frequency response curve Ω is a control parameter. In Duffing and quadratic oscillators β_0 and β_1 are non-dimensional parameters, so values of these coefficients affect significantly on response of system.

Arrange the constitutive equations (Eqs. (3.3)) in following form,

$$\begin{aligned}\ddot{x} &= \gamma \cos(\Omega t) - (x - \text{sgn}(x)\lambda\xi) - 2\zeta\dot{x} - \beta_0 x^3 - \beta_1 x^2, \\ \dot{\vartheta} &= h(\vartheta_E - \vartheta) - Z_2 \dot{\xi}\end{aligned}\tag{3.4}$$

So using set of Eqs. (3.4) follow a harmonic balance method as mentioned in Chapter 2 and obtained a harmonic balance equations. Using that equations obtained a frequency response curves for displacement and temperature.

3.2.3 Result and Discussion

In model, SMA device shows nonlinear behavior due to energy dissipation capability. Duffing oscillator and quadratic oscillator have cubic and quadratic non-linearity respectively. Combine of these two oscillator with SMA device shows a peculiar behavior. For investigation and analysis obtained a frequency response curves of both displacement and temperature. The whole system contained three oscillator: SMA oscillator, Duffing oscillator and quadratic oscillator. The material of SMM device keep as Ni-Ti alloy.

In non-isothermal regime ($\dot{\vartheta} \neq 0$), so model consider a thermodynamic parameter as given by Eq. (3.4). SMA has a strong coupling between thermal and mechanical parameters. The same values of parameters are used as mentioned in isothermal case of shape memory devices. The

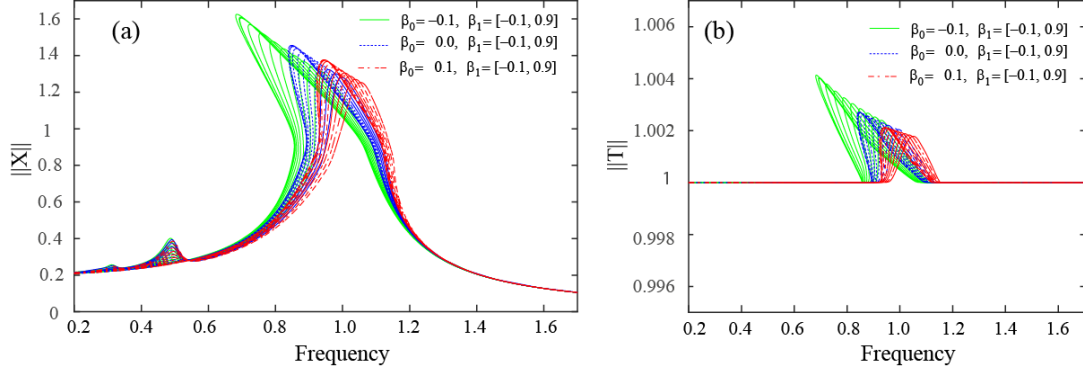


Figure 3.2: (a)Frequency response curves of SMA based cubic and quadratic oscillators for displacement in non-isothermal case (b)Frequency response curves of SMA based cubic and quadratic oscillators for temperature in non-isothermal case

Duffing oscillator and quadratic oscillator added to SMA device and due to combination of Duffing and quadratic oscillators behavior of SMA device affected. The cubic and quadratic non-linearity of Duffing and quadratic oscillators affect on both displacement and temperature behavior of system. The response of Duffing and quadratic oscillators are defined by $\beta_0 x^3$ and $\beta_1 x^2$ terms respectively so values of β_0 and β_1 have significant impact on response of system. Addition of Duffing and quadratic oscillators in system of SMA device produce complex behavior. Investigation of this complex behavior is useful in industrial applications. Such a complex response captured in frequency response curves and resonance frequency of system is observed.

In SMA system frequency response curves shows softening nature for both displacement and temperature. Addition of quadratic oscillator, add some different result in frequency response curves. The model of SMA device with Duffing and quadratic oscillators used same parameter as mentioned in isothermal case of SMA device in Chapter 2. In this thesis, Duffing coefficient (β_0) kept constant and vary quadratic coefficient (β_1) from -0.1 to 0.9 to study the effect of quadratic oscillator. In Figure 3.2(a) and Figure 3.2(b) green curves drawn at $\beta_0 = -0.1$, blue curves at $\beta_0 = 0$ and red curves at $\beta_0 = 0.1$, here vary β_1 from -0.1 to 0.9 at each β_0 value. The combination of two oscillator with SMA device shows partial effect of Duffing oscillator and partial effect of quadratic oscillator. The system with quadratic oscillator shows superharmonic response. It also affect the softening nature of SMA system. But influence of of quadratic oscillator on softening nature of SMA damping system is less compared to Duffing oscillator. For low value of β_1 i.e $\beta_1 = -0.1$ to 0.2 frequency response curve shows very less superharmonic response. For $\beta_1 = 0.3$ or more than that frequency response curve shows higher influence of superharmonic response. Here superharmonic response is linear. But simultaneously Duffing coefficient also has a effect on system and combination of these two oscillator convert softening nature to hardening nature. If Duffing coefficient kept constant and only vary the quadratic coefficient then it is found that all curves meet at single point near to superharmonic region and orientation of further curve remains same as response of SMA device with Duffing oscillator. That concurrent single point shift towards higher frequency with increase of Duffing coefficient. The superharmonic response found only in displacement frequency response curves. Similar type of response also found in temperature frequency response curves. With the increase of value of both coefficients (β_0 & β_1) nature of curve changes from softening to linear to

hardening. With increase of a value of quadratic coefficient peak of superharmonic region increases. As shown in Figure 3.2(a), with increase of value of β_1 peak of superharmonic region increases and initiation of adjacent superharmonic region (left side). At higher values of both coefficients frequency response curves indicate hardening nature.

3.3 Summary

The Duffing oscillator governed by cubic term of displacement which has significant impact on response of SMA system. The Duffing oscillator directly affecting on softening nature of SMA devices. The value of Duffing coefficient decide the nature of Duffing oscillator. The comparison of Duffing oscillator between with SMA and without SMA describe the influence of SMA device on Duffing oscillator. In this section analysis of SMA device with Duffing and quadratic oscillator contribute the study to non-linear dynamics. With quadratic and cubic oscillator SMA device has partial influence of both oscillators. Quadratic oscillator is responsible for linear superharmonic region. Both coefficients: quadratic coefficient and Duffing coefficient has a significant influence on SMA device. The system has complex behavior and study of this behavior useful in industrial applications.

Chapter 4

Analysis of SMA Model by Method of Averaging

In this Chapter, we describe the method of averaging [23] to obtain the nonlinear response and compare the same with the method of harmonic balance. To present the comparison, we take the SMA based oscillator with or without cubic nonlinearity under isothermal condition.

4.1 Mathematical Model

The mathematical model of SMA system obtained in Chapter 2. The same constitutive equations used as obtained in discussion of mathematical model for SMA system. The non-dimensional form of constitutive equations used for method of averaging. For the sake of convenience write a set of constitutive equations again,

$$\dot{x} = v,$$

$$\dot{v} = \gamma \cos(\Omega t) - (x - \text{sgn}(x)\lambda\xi) - 2\zeta v,$$

$$\dot{\xi} = \frac{Z_1}{1 - Z_1 Z_2} [\text{sgn}(x)Jv + h(\vartheta - \vartheta_E)],$$

$$\dot{\vartheta} = \frac{1}{1 - Z_1 Z_2} [-\text{sgn}(x)JZ_1 Z_2 v - h(\vartheta - \vartheta_E)]. \quad (4.1)$$

This set of equations used in method of averaging and equations obtained from method of averaging used for plotting the frequency response curves.

4.2 A Numerical Method: Method of Averaging

In the study of dynamical systems, the method of averaging based on Krylov–Bogolyubov method of averaging [23] is used to study certain time-varying systems. This is a mathematical method for approximate analysis of oscillating processes in non-linear mechanics. The method of averaging is a useful computational technique to obtain an approximate solution of non-linear differential equations. This method is based on the averaging principle which replaced exact differential equations by averaged equations. In order to validate the system behavior, the method of averaging is used to obtain the frequency response curves.

Arrange the constitutive equations Eqs. (4.1) as follows,

$$\begin{aligned}\ddot{x} &= \gamma \cos(\Omega t) - (x - \operatorname{sgn}(x)\lambda\xi) - 2\zeta\dot{x}, \\ \dot{\vartheta} &= h(\vartheta_E - \vartheta) - Z_2\dot{\xi}\end{aligned}\tag{4.2}$$

Apply the method of averaging to the first constitutive equation of the set of Eqs. (4.2),

$$\ddot{x} = \gamma \cos(\Omega t) - (x - \operatorname{sgn}(x)\lambda\xi) - 2\zeta\dot{x},$$

consider, $f(x, \vartheta) = (x - \operatorname{sgn}(x)\lambda\xi)$, so the constitutive equation becomes,

$$\ddot{x} = \gamma \cos(\Omega t) - f(x, \vartheta) - 2\zeta\dot{x},\tag{4.3}$$

Let us assume,

$$x = R \cos(\Omega t + \Phi)$$

where R is amplitude and Φ is phase, both are slow varying with respect to time. Consider $\theta = \Omega t + \Phi$.

$$x = R \cos(\Omega t + \Phi) = R \cos(\theta)\tag{4.4}$$

Differentiating Eq. (4.4) with respect to time, yield

$$\begin{aligned}\dot{x} &= \dot{R} \cos(\Omega t + \Phi) - \Omega R \sin(\Omega t + \Phi) - \dot{\Phi} R \sin(\Omega t + \Phi) \\ \dot{x} &= \dot{R} \cos(\theta) - \Omega R \sin(\theta) - \dot{\Phi} R \sin(\theta)\end{aligned}\tag{4.5}$$

making,

$$\dot{R} \cos(\theta) - \dot{\Phi} R \sin(\theta) = 0\tag{4.6}$$

Eq. (4.5) becomes as following,

$$\dot{x} = -\Omega R \sin(\theta)\tag{4.7}$$

Differentiating Eq. (4.7) with respect to time, yield

$$\ddot{x} = -\Omega \dot{R} \sin(\Omega t + \Phi) - \Omega^2 R \cos(\Omega t + \Phi) - \dot{\Phi} R \sin(\Omega t + \Phi)$$

$$\ddot{x} = -\Omega \dot{R} \sin(\theta) - \Omega^2 R \cos(\theta) - \dot{\Phi} R \sin(\theta) \quad (4.8)$$

Substitute Eq. (4.7) and Eq. (4.8) in Eq. (4.3), yield

$$-\Omega \dot{R} \sin(\theta) - \Omega^2 R \cos(\theta) - \dot{\Phi} R \sin(\theta) + f(x, \vartheta) - 2\Omega \zeta R \sin(\theta) = \gamma \cos(\Omega t) \quad (4.9)$$

Solving Eq. (4.6) and Eq. (4.9) for \dot{R} and $\dot{\Phi}$, obtained

$$\dot{R} = \frac{-\gamma \cos(\Omega t) \sin(\theta)}{\Omega} - \Omega R \sin(\theta) \cos(\theta) - 2\zeta R \sin^2(\theta) + \frac{f(x, \vartheta) \sin(\theta)}{\Omega} \quad (4.10)$$

$$\dot{\Phi} = \frac{-\gamma \cos(\Omega t) \cos(\theta)}{\Omega R} - \Omega \cos^2(\theta) - 2\zeta \sin(\theta) \cos(\theta) + \frac{f(x, \vartheta) \cos(\theta)}{\Omega R} \quad (4.11)$$

The above Eq. (4.10) and Eq. (4.11) can be averaged over one cycle of θ . In these equations R and Φ are slowly varying compare to θ so assume R and Φ as constants. By averaging equations are,

$$\dot{R} = \frac{1}{2\pi} \int_0^{2\pi} \left(\frac{-\gamma \cos(\Omega t) \sin(\theta)}{\Omega} - \Omega R \sin(\theta) \cos(\theta) - 2\zeta R \sin^2(\theta) + \frac{f(x, \vartheta) \sin(\theta)}{\Omega} \right) d\theta \quad (4.12)$$

$$\dot{\Phi} = \frac{1}{2\pi} \int_0^{2\pi} \left(\frac{-\gamma \cos(\Omega t) \cos(\theta)}{\Omega R} - \Omega \cos^2(\theta) - 2\zeta \sin(\theta) \cos(\theta) + \frac{f(x, \vartheta) \cos(\theta)}{\Omega R} \right) d\theta \quad (4.13)$$

Solution of Eq. (4.12) and Eq. (4.13) are,

$$\dot{R} = \frac{-\gamma \sin(\Phi)}{2\Omega} - \zeta R + \frac{1}{2\pi} \int_0^{2\pi} \left(\frac{f(x, \vartheta) \sin(\theta)}{\Omega} \right) d\theta \quad (4.14)$$

$$\dot{\Phi} = \frac{-\gamma \cos(\Phi)}{2\Omega R} - \frac{\Omega}{2} + \frac{1}{2\pi} \int_0^{2\pi} \left(\frac{f(x, \vartheta) \cos(\theta)}{\Omega R} \right) d\theta \quad (4.15)$$

These above equations (Eq. (4.12) and Eq. (4.13)) are output of method of averaging. These differential equations of R and Φ are used to plot frequency response curves of amplitude and phase respectively. To plot frequency response curves solve these equations at equilibrium.

At equilibrium,

$$\dot{R} = \frac{-\gamma \sin(\Phi)}{2\Omega} - \zeta R + \frac{1}{2\pi} \int_0^{2\pi} \left(\frac{f(x, \vartheta) \sin(\theta)}{\Omega} \right) d\theta = 0 \quad (4.16)$$

$$\dot{\Phi} = \frac{-\gamma \cos(\Phi)}{2\Omega R} - \frac{\Omega}{2} + \frac{1}{2\pi} \int_0^{2\pi} \left(\frac{f(x, \vartheta) \cos(\theta)}{\Omega R} \right) d\theta = 0 \quad (4.17)$$

For solving integration term in equilibrium equation, assume Fourier series as,

$$f(x, \vartheta) = \frac{y_0}{2} + \sum_{i=1}^N U_n \cos(n\Omega t) + V_n \sin(n\Omega t) \quad n = 1, 2, \dots, N$$

$$f(x, \vartheta) = \frac{y_0}{2} + \sum_{i=1}^N U_n \cos(n(\theta - \Phi)) + V_n \sin(n(\theta - \Phi)) \quad n = 1, 2, \dots, N \quad (4.18)$$

Substitute Eq. (4.18) in Eq. (4.16) and Eq. (4.17), yield equilibrium equations by solving integration terms. In final form of equilibrium equations U_n and V_n are Fourier coefficients, to calculate these Fourier coefficients use the iterative algorithm based on the evaluation of R and Φ . From values of R and Φ calculate values of x for timespan of $[0 \frac{2\pi}{\Omega}]$. In isothermal case ϑ is constant. Using values of x and ϑ obtained the values of ξ by using numerical integration. Obtained the values of $f(x, \vartheta)$ using values of x , ϑ and ξ . Finally, calculate the values of U_n and V_n by using IFFT (Inverse Fast Fourier Transform). In order to obtained a unstable branch of frequency response curve used arc continuation method. Here, spherical arclength continuation method is used to obtained a constrained equation. The constrained equation are as follows,

$$(\mathbf{x} - \mathbf{x}_i)^T (\mathbf{x} - \mathbf{x}_i) - (\Delta s)^2 = 0$$

Here, \mathbf{x} is unknown quantity of current step and \mathbf{x}_i known quantity of previous step. In above constrained equation s is arclength along a curve and Δs is step size. In this thesis, predictor-corrector algorithm is used for iterative method. Here, secant predictor algorithm used and proposed as following,

$$\mathbf{x}_{i+1} = \mathbf{x}_i + p_i (\mathbf{x}_i - \mathbf{x}_{i-1})$$

Where, p_i is step-dependent parameter. For corrector algorithm used Newton-Raphson iterative method and by using predictor-corrector method obtained values of unknown constant.

4.3 Result and Discussion

The investigation and detailed study of SMA devices was done in Chapter 2 with frequency response curves. To draw frequency response curves various numerical methods are used. These methods are multiple scale method, method of averaging and harmonic balance method etc. In Chapter 2 frequency response curves are obtained by using harmonic balance method, to validate these frequency response curves implement method of averaging on same constitutive equations. The material of SMM device keep as Ni-Ti alloy.

4.3.1 SMA Oscillator without Cubic Nonlinearity

The behavior of system and implications of frequency response curves studied in Chapter 2. In isothermal case, temperature is constant, so investigation deals with only displacement frequency response curves. In method of averaging, values of non-dimensional parameters keep same as men-

tioned in isothermal case of Chapter 2. By using method of averaging obtained the displacement frequency response curves as shown in Figure 4.1(a). The comparison of results between harmonic balance method and method of averaging shown in Figure 4.1(c). The variation between results obtained by two methods are very small. Here variation occur because of procedures followed by these methods and difference in numerical solutions. In numerical method, selection of initial values,

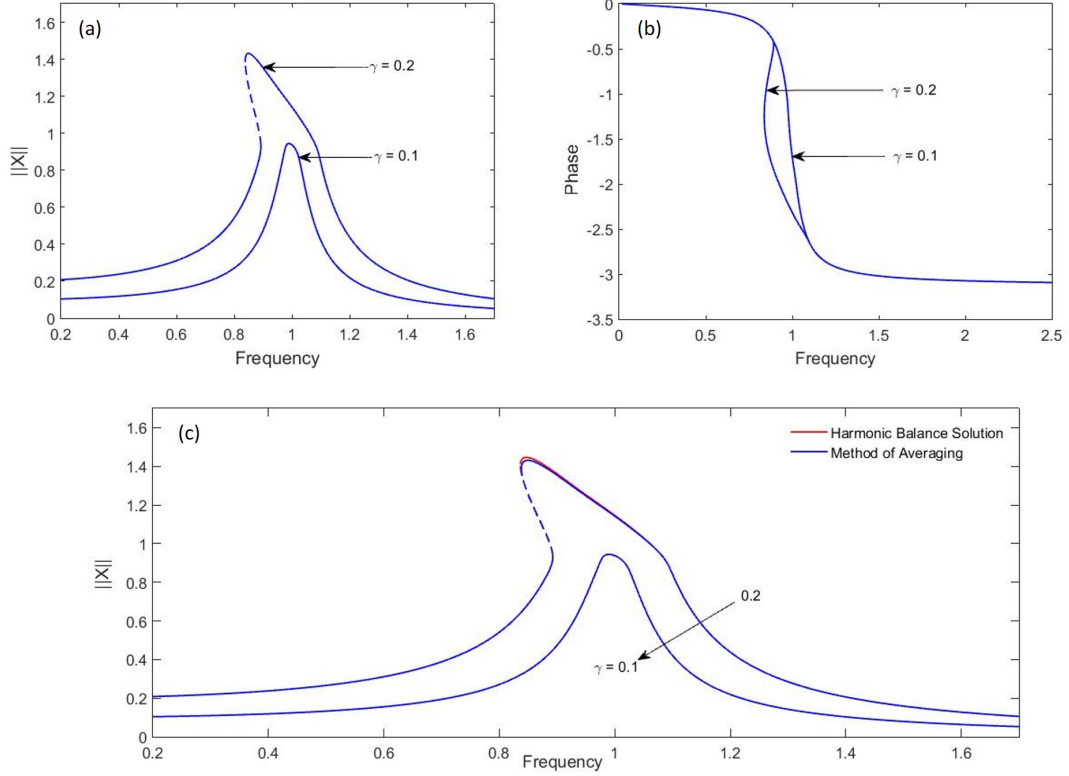


Figure 4.1: (a)Frequency response curves of SMA for displacement in non-isothermal case by method of averaging (b)Frequency response curves of SMA for temperature in non-isothermal case (c)Comparison of frequency response curves of SMA for displacement between harmonic balance solution and method of averaging in non-isothermal case ($\gamma = 0.2$)

tolerance limit, method used for continuation of bifurcation points and method of predictor-corrector etc. factors have influence on graph plotting in MATLAB [24]. So because of these factors variations occur between results obtained by these two methods. For $\gamma = 0.1$ i.e for low forcing there is no variation in results of these two methods. The very small variation occur for higher forcing ($\gamma = 0.2$). The amount of variations is slightly high in higher forcing because of various factors influence on plotting of frequency response curve in MATLAB. The difference between two results are (for $\gamma = 0.2$), peak of curve is high in harmonic balance solution than method of averaging and resonance frequency is slightly less in harmonic balance solution than method of averaging. Figure 4.1(c) shows that nature and values of curves are nearly same and variations are very small. So by using this reference, validate the result of harmonic balance method by using the method of averaging.

In method of averaging two differential equations obtained for amplitude and phase. In Figure 4.1(a) and Figure 4.1(c) results obtained from solution for amplitude are shown. The solution of

differential equation for phase give a phase frequency response curve. The phase frequency response curve shown in Figure 4.1(b). It can be seen that the phase is distorted by the nonlinearity to exhibit a multivalued region. Also, same method is used to plot frequency response curves for phase as used for amplitude. Two frequency response curves of phase at different excitation amplitudes $\gamma = 0.1$ and $\gamma = 0.2$. At -90° curve changes its response. It can also be found that, as the excitation frequency increases, the non-linearity exhibited in plots and for low frequencies it disappeared.

4.3.2 SMA Oscillator with Cubic Nonlinearity

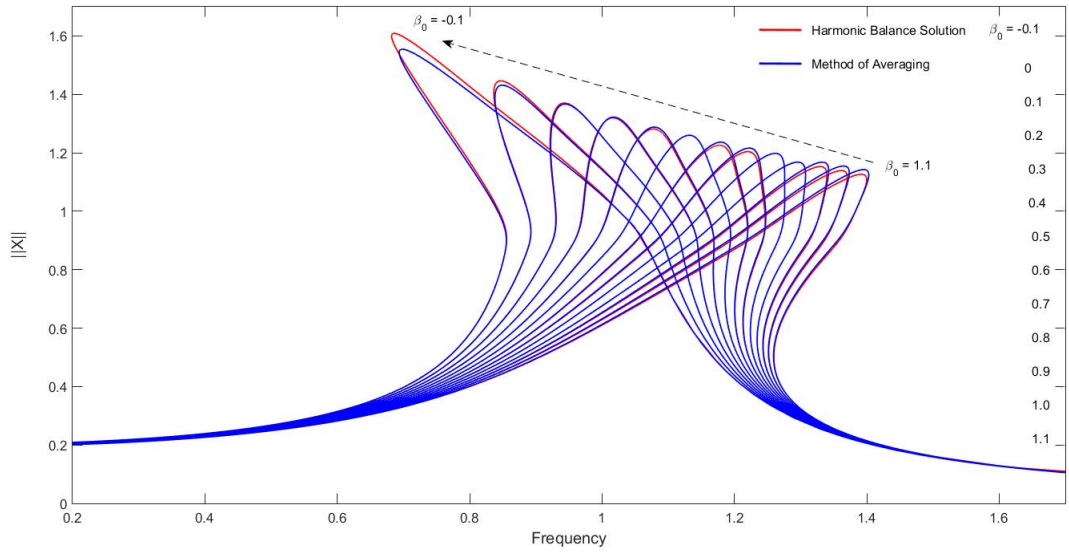


Figure 4.2: Comparison of frequency response curves of SMA based cubic oscillator for displacement between harmonic balance solution and method of averaging in isothermal case ($\gamma = 0.2$)

Method of averaging [23] applied to SMA based cubic oscillator to obtained a frequency response curves for displacement. In Eq. (4.3) expression of $f(x, \vartheta)$ taken as $f(x, \vartheta) = (x - \text{sgn}(x)\lambda\xi + \beta_0x^3)$, cubic term added in expression. In Figure 4.2 blue curves drawn by method of averaging and red curves drawn by harmonic balance solution. Frequency response curves drawn for range of $\beta_0 = -0.1$ to 1.1 by both methods. Comparison between two methods is necessary to find the most correct approximation methods suitable for SMA based cubic oscillator. From Figure 4.2, it is found that difference between two method is very less. This difference is occur due to tolerance difference or initial values or method of numerical integration. But for some curves response by two methods are exactly matching. In this way we can state that both approximation method giving almost correct results.

4.4 Summary

The behavior of SMA device is investigated by frequency response curves obtained using the method of averaging and harmon balance method. It is found that the averaging method underestimate the results as compared to the method of harmonic balance. However, both the methods can be used to study the influence of forcing on the response of SMA based oscillators.

Chapter 5

Conclusion and Future work

5.1 Conclusion

In this thesis, we present the governing equation to describe the thermomechanical behavior of shape-memory alloys (SMA) using the equation of motion and the constitutive equation of SMA under isothermal and non-isothermal condition. Subsequently, we discuss the method of harmonic balance to solve the coupled equation to obtain the linear and nonlinear frequency response. After validating the solution obtained by harmonic balance method with the numerical solution and the available results in the literature, we obtain the solution under isothermal and non-isothermal conditions.

To analyze the influence of cubic and quadratic nonlinear stiffness on the response of SMA based oscillator, we add the nonlinear terms in the governing equation and solve it using the method of harmonic balance under non-isothermal condition. On comparing the results, we found that by varying the coefficient of cubic and quadratic nonlinearity, the frequency response of SMA based oscillator can be tuned effectively. Subsequently, we also present the method of averaging to obtain nonlinear frequency response of SMA based oscillator under isothermal condition with and without cubic nonlinearity. On comparing the solutions obtained from the method of harmonic balance and the method of averaging, we found that the averaging solution underestimate the results. Finally, we state that we have presented different solution methods to obtain the nonlinear frequency response of SMA based oscillator with or without cubic and quadratic oscillators under isothermal as well as non-isothermal condition. It can be used in analyzing the SMA based phenomena in varieties of applications.

5.2 Future work

The methods presented in the thesis in analyzing SMA based oscillators are based on single time scale. To analyze the relative importance of time scale associated with beam resonator and SMA, we can employ more general approach based the method of multiple scale. Moreover, a typical experimental studies can also be performed to capture the above effects accurately.

References

- [1] K. Otsuka and C. M. Wayman. Shape memory materials. Cambridge university press, 1999.
- [2] C. L. Dimitris. Shape memory alloys: Modeling and engineering applications 2008.
- [3] D. Bernardini and F. Vestroni. Non-isothermal oscillations of pseudoelastic devices. *International Journal of Non-Linear Mechanics* 38, (2003) 1297–1313.
- [4] W. Lacarbonara, D. Bernardini, and F. Vestroni. Nonlinear thermomechanical oscillations of shape-memory devices. *International Journal of Solids and Structures* 41, (2004) 1209–1234.
- [5] D. Bernardini and G. Rega. The influence of model parameters and of the thermomechanical coupling on the behavior of shape memory devices. *International Journal of Non-Linear Mechanics* 45, (2010) 933–946.
- [6] D. Bernardini. On the macroscopic free energy functions for shape memory alloys. *Journal of the Mechanics and Physics of Solids* 49, (2001) 813–837.
- [7] Y. Ivshin and T. J. Pence. A thermomechanical model for a one variant shape memory material. *Journal of intelligent material systems and structures* 5, (1994) 455–473.
- [8] M. O. Moussa, Z. Moumni, O. Doaré, C. Touzé, and W. Zaki. Non-linear dynamic thermo-mechanical behaviour of shape memory alloys. *Journal of Intelligent Material systems and structures* 23, (2012) 1593–1611.
- [9] J. Salichs, Z. Hou, and M. Noori. Vibration suppression of structures using passive shape memory alloy energy dissipation devices. *Journal of Intelligent Material Systems and Structures* 12, (2001) 671–680.
- [10] P. Thomson, G. Balas, and P. Leo. The use of shape memory alloys for passive structural damping. *Smart Materials and Structures* 4, (1995) 36.
- [11] P. W. Clark, I. D. Aiken, J. M. Kelly, M. Higashino, and R. Krumme. Experimental and analytical studies of shape-memory alloy dampers for structural control. In *Smart Structures & Materials' 95*. International Society for Optics and Photonics, 1995 241–251.
- [12] M. Urabe. Galerkin's procedure for nonlinear periodic systems. *Archive for Rational Mechanics and Analysis* 20, (1965) 120–152.
- [13] A. H. Nayfeh and B. Balachandran. Applied nonlinear dynamics: analytical, computational, and experimental methods. In *Wiley Series in Nonlinear Sciences*. John Wiley & Sons, Inc New York, 1995.

- [14] N. Van Dao and E. J. Kreuzer. IUTAM Symposium on Recent Developments in Non-linear Oscillations of Mechanical Systems: Proceedings of the IUTAM Symposium Held in Hanoi, Vietnam, March 2–5, 1999, volume 77. Springer Science & Business Media, 2012.
- [15] G. Ge. Response of a Shape Memory Alloy Beam Model under Narrow Band Noise Excitation. *Mathematical Problems in Engineering* 2014.
- [16] F. Vestroni and D. Capecchi. Coupling and resonance phenomena in dynamic systems with hysteresis. In IUTAM Symposium on New Applications of Nonlinear and Chaotic Dynamics in Mechanics. Springer, 1999 203–212.
- [17] S. Saadat, J. Salichs, M. Noori, Z. Hou, H. Davoodi, I. Bar-On, Y. Suzuki, and A. Masuda. An overview of vibration and seismic applications of NiTi shape memory alloy. *Smart materials and structures* 11, (2002) 218.
- [18] E. Oberaigner, K. Tanaka, and F. Fischer. Investigation of the damping behavior of a vibrating shape memory alloy rod using a micromechanical model. *Smart materials and structures* 5, (1996) 456.
- [19] B. Raniecki, C. LExcellent, and K. Tanaka. Thermodynamic models of pseudoelastic behaviour of shape memory alloys. *Archiv of Mechanics, Archiwum Mechaniki Stosowanej* 44, (1992) 261–284.
- [20] I. Kovacic and M. J. Brennan. The Duffing equation: nonlinear oscillators and their behaviour. John Wiley & Sons, 2011.
- [21] A. H. Nayfeh and N. E. Sanchez. Bifurcations in a forced softening Duffing oscillator. *International Journal of Non-Linear Mechanics* 24, (1989) 483–497.
- [22] H. Hu. Solution of a quadratic nonlinear oscillator by the method of harmonic balance. *Journal of Sound and Vibration* 293, (2006) 462–468.
- [23] N. M. Krylov and N. N. Bogoliubov. Introduction to Non-Linear Mechanics.(AM-11), volume 11. Princeton University Press, 2016.
- [24] J. Stoer and R. Bulirsch. Introduction to numerical analysis, volume 12. Springer Science & Business Media, 2013.
- [25] L. Cveticanin. Vibrations of the nonlinear oscillator with quadratic nonlinearity. *Physica A: Statistical Mechanics and its Applications* 341, (2004) 123–135.